ULTRASTRUCTURE OF APLANOSPORE PRODUCTION AND GERMINATION AND THE ROLE OF CALCIUM IN GERMINATION OF APLANOSPORES OF *VAUCHERIA LONGICAULIS* VARIETY *MACOUNII* BLUM (CHRYSOPHYTA, TRIBOPHYCEAE)

by

ROBERT SCOTT FITCH

B.A., UNIVERSITY OF CALIFORNIA, SANTA BARBARA, 1980

A THESIS SUBMITTED IN PARTIAL FULFILMENT OF
THE REQUIREMENTS FOR THE DEGREE OF
MASTERS OF SCIENCE

in

THE DEPARTMENT OF BOTANY

We accept this thesis as conforming
to the required standard

THE UNIVERSITY OF BRITISH COLUMBIA

August 1986

In presenting this thesis in partial fulfilment of the requirements for an advanced degree at the University of British Columbia, I agree that the Library shall make it freely available for reference and study. I further agree that permission for extensive copying of this thesis for scholarly purposes may be granted by the head of my department or by his or her representatives. It is understood that copying or publication of this thesis for financial gain shall not be allowed without my written permission.

Department of BOTANY

The University of British Columbia
1956 Main Mall
Vancouver, Canada
V6T 1Y3

Date SEPTEMBER 30, 1986

Vaucheria longicaulis var. *macounii* (Blum) is the most common of the four brackish water species of *Vaucheria* known to occur in British Columbia and northern Washington. This variety is easy to maintain in culture with minimum nutritional requirements. It survives culture conditions for extended periods of time (up to 2 years or more) without losing its reproductive capabilities. Aplanosporogenesis is easily induced by transferring plants to fresh medium with almost every vegetative filament producing one apical aplanosporangium containing a single aplanospore.

Aplanosporogenesis has been examined in sections prepared for light and electron microscopies. As the vegetative filament tip expands, signalling the beginning of aplanosporogenesis, the large central vacuole is displaced from the tip. An inner wall is secreted within the existing cell wall via exocytosis of numerous fibrillar-containing vesicles. Septation of the aplanosporangium from the vegetative filament is accomplished by the centripetal infurrowing of this newly secreted inner wall at the base of the enlarged filament tip. Each aplanosporangium produces a single, multinucleated walled aplanospore, with unique organelle morphologies and associations. The importance of these organelles in the mechanism of aplanospore

release and germination are discussed.

Germination of aplanospores is initiated at sites characterized by low optical density and leads to the formation of filaments. The most prominent ultrastructural features characterizing germination are the rapid expansion of the central vacuole, the accumulation of dictyosome-derived vesicles at the tip of the germinating filament in association with cell wall expansion, and the increase in the number and redistribution of microtubules. The possible function of unique organelle associations, such as those occurring among the mitochondria-endoplasmic reticulum-dictyosome association, are discussed as well. In addition, quantitative changes in the volume density of some subcellular compartments and organelles are evaluated using morphometric analysis.

Using the fluorescent probe chlorotetracycline as an indicator of intracellular Ca^{2+}, the role(s) of calcium on aplanospore germination and filament growth are studied. These studies are supplemented with the use of drugs to disrupt the availability and distribution of extra- and intracellular Ca^{2+}. The results are then analyzed in terms of the complexities of the mechanisms involved in the germination and growth of *Vaucheria* aplanospores.

LIST OF TABLES

LIST OF FIGURES

FIGURE

ACKNOWLEDGEMENTS

The author gratefully acknowledges the financial support and the insightful guidance of Dr. L. Oliveira, his thesis supervisor. His patience, encouragement and wisdom were invaluable in the completion of this work. He wishes to thank Dr. T. Bisalputra for full and unrestricted use of all his research facilities during the course of this study. Sincere gratitude is also extended to Dr. M. Hawkes and Dr. D. Garbary; their phycological insights and academic enthusiasm were contagious. He also expresses heartfelt gratitude to office partners and fellow students whose friendships, laughter and support helped realize this thesis.

Most importantly, he thanks his wife, Kathy, whose unceasing love, patience and commitment kept him going.

Vaucheria is a widely distributed algal genus occurring in both freshwater and marine habitats. In temperate regions it is a common floral element in salt marshes and estuaries. *Vaucheria* has been a generally overlooked member of the marine algal flora of British Columbia and northern Washington. In a comprehensive list of marine algae from the area, Scagel (1957) included *V. litorea* (Agardh) based on the earlier report of Jao (1937) and an additional personal collection. Blum (1971) later described *V. longicaulis* var. *macounii* and *V. intermedia* (Nordstadt) from northern Washington, and later referred to *V. thuretii* (Woronin) from the Pacific coast of the United States (Blum, 1972). In addition, Pomeroy (1977) and Pomeroy and Stockner (1976) report *V. dichotoma* (Agardh) from British Columbia. For a general review of the ecology and distribution of marine/brackish *Vaucheria* spp., see Simons (1975).

The genus *Vaucheria* has been widely studied since the plants were first described by Vaucher (1801). Asexual reproduction is accomplished by means of akinetes, multiflagellated zoospores or non-motile aplanospores depending upon the species (Venkataraman 1961, Blum 1972, Rieth 1980). Previous ultrastructural studies have dealt with the vegetative filament (Ott and Brown 1974a, Ott 1979), mitosis (Ott and Brown, 1972),

spermatogenesis (Moestrup 1970, Ott and Brown 1978) and the chloroplast (Dangeard 1939, Descomps 1963a, 1963b, Marchant 1972). Uniquely multiflagellated and multinucleated zoospores and zoosporogenesis have been extensively studied by light (Trentephol 1807, Unger 1843, Thuret 1843, Pringsheim 1855, Schmitz 1878, Strasburger 1880, 1890, Koch 1951) and electron microscopies (Greenwood *et al* 1957, Greenwood 1959, Ott and Brown 1974b, 1975).

Despite the fact that aplanospores are reported in approximately twice as many species of *Vaucheria* as are zoospores, information on aplanosporogenesis, release and subsequent germination of aplanospores is only very briefly dealt with by Fritsch (1935), Smith (1950), Taylor (1952), Chopra (1971), Knutzen (1973), Simons (1974) and Garbary and Fitch (1984). However, none of these studies involved ultrastructural work. In a portion of this thesis, therefore, the events leading to the differentiation of the vegetative filament apex into the aplanospore will be reported. The mechanism of aplanospore release and the ultrastructural events characterizing aplanospore germination in *V. longicaulis* var. *macounii* will also be studied. In addition, morphometric analysis is used to quantify the ultrastructural events occurring in aplanospores during

the early stages of germination.

Recent studies emphasize that Ca^{2+} ions play many important roles in cellular growth processes in plants (see Quatrano 1978, Weisenseel and Kicherer 1981, Sievers and Schnepf 1981, Polito 1985 and Marmé 1985 for reviews). Plant cell processes regulated by Ca^{2+} ions include bud formation (Saunders and Hepler 1981, Saunders 1986), cytoplasmic viscosity (Picton and Steer 1982, Goodwin and Trainor 1985), mitosis (Wolniak *et al* 1980, Saunders and Hepler 1981, Hepler and Wayne 1985), wound healing in giant algal cells (La Claire, 1983, 1984), cell volume (Kauss and Rausch, 1984) and recovery from freezing injury (Woods *et al*, 1984).

Vaucheria is a coenocytic alga in which germination and subsequent filament growth is initiated by oriented exocytosis of dictyosome-derived vesicles at specific regions along the aplanospore (Fitch and Oliveira, 1986b) and at the tip of the growing filament (Ott and Brown 1974, 1975a, 1975b, Kataoka 1982, Fitch and Oliveira 1986a, 1986b).

Control of polarized growth of pollen tubes is known to involve tip-localized Ca^{2+} concentration gradients arising from the influx of Ca^{2+} ions across membranes (Quatrano 1978, Chen and Jaffe 1979, Weisenseel and Kicherer 1981, Polito 1985). These

gradients have been reported in many other tip-growing plant and fungal cells and are known to sustain oriented exocytosis of polysaccharide-storing vesicles necessary for apical wall expansion and subsequent growth (Jaffe *et al* 1975, Herth 1978, Quatrano 1978, Reiss and Herth 1978, 1979a, 1979b, 1982, Saunders and Hepler 1981, Weisenseel and Kicherer 1981, Meindl 1982, Picton and Steer 1982, 1985, Hausser and Herth 1983, Reiss *et al* 1983, 1985, Goodwin and Trainor 1985, Polito 1985, Wayne and Hepler 1985, McKerracher and Heath 1986). The distribution of cellular organelles in pollen tubes also seems to be regulated by a tip-localized distribution of Ca^{2+} ions (Weisenseel and Kicherer 1981, Meindl 1982, Picton and Steer 1982, Reiss and Herth 1982, Grotha 1983). Cytoplasmic Ca^{2+} is also known to participate in the regulation of cytoplasmic streaming in algae (Hepler and Wayne, 1985) and fungal cells (McKerracher and Heath, 1986).

The fluorescent probe chlorotetracycline (CTC) has often been used as an indicator of membrane-bound Ca^{2+} in living cells (for a review see Caswell, 1979). By employing CTC to localize intracellular Ca^{2+} and combining this data with ultrastructural observations of germination in *Vaucheria*, an attempt is made to present an integrated picture of the role of Ca^{2+} in the complex

mechanism of polarized germination and filament extension in V. longicaulis var. macounii.

Calcium is also known to be involved in the regulation of the viscoelasticity of the gel-like cytoplasm rich in cytoskeletal elements found adjacent to the plasma membrane (Goodwin and Trainor, 1985). Overall, the polarizing capacity of the peripheral cytoplasm is thought to be based on the formation of ion gradients and electrical potential differences with Ca^{2+} ions playing a major role in this system (Schnepf, 1986). Local variations in calcium distribution are, therefore, part of the mechanism affecting localized growth in plant cells (Picton and Steer 1982, Goodwin and Trainor 1985).

By using specific drugs it is possible to interfere with both extra- and intracellular Ca^{2+} availability and distribution; hence to ascertain some aspects of the involvement of these ions in tip-oriented growth. Therefore, perturbations in the intracellular balance of Ca^{2+}, caused by the drugs ethyleneglycoltetraacetic acid (EGTA), calcium ionophore A23187 and trifluoperazine (TFP), are discussed in terms of those mechanisms known to participate in tip-oriented growth in Vaucheria.

Vaucheria spp. were collected primarily in Mud Bay (Blackie's Spit), the Fraser River estuary, Vancouver Harbor (Burrard Inlet) and the Strait of Georgia in southern British Columbia. Most collections were made in salt marshes where *Vaucheria* spp. grow at the bases of, or in bare patches among *Salicornia virginica* and various other estuarine phanerogams. *Vaucheria* spp. produced dense mats from several centimeters to many meters in lateral extent.

Plants were returned to the laboratory for identification. Venkataraman (1961), Blum (1972) and Rieth (1980) were the primary taxonomic authorities. If plants were sterile, portions of the algal mats were placed in glass petri dishes and moistened with culture media. Cultures usually became reproductive within one month. Portions of reproductive mats were mounted for deposit in the University of British Columbia Herbarium (UBC) or fixed with 5% formalin and maintained in liquid preservative (70% ethanol).

Vaucheria spp. have been maintained in culture for as long as one and one half years. Media utilized was half strength Instant Ocean (Aquarium Systems Inc., Eastlake, Ohio) supplemented with minor elements (Lewin, 1966) and soil extract. Cultures were kept at 10°C, with cool white light of photon flux density of *ca*. 25

umol m^{-2} s^{-1} under a 16-8 h light-dark photoperiod.

Cultures of V. longicaulis var. macounii were transferred into fresh media to induce aplanosporogenesis. This usually occurred within 24 hours. Observations of aplanosporogenesis and aplanospore germination using living material were made with a Leitz Dialux 20 EB compound light microscope. Growth of filaments germinating from aplanospores was recorded using a Wild MPS 11 dissecting microscope equipped with an eyepiece micrometer.

For ultrastructural studies, freshly collected aplanospores and germinating filaments were placed in 1% (v/v) glutaraldehyde made from an 8% stock solution (Polysciences Inc., Warrington, PA), buffered in 0.1 M phosphate buffer saline (PBS), pH 6.9, for 45 minutes at room temperature (20-23°C). After transfer to a final solution of 4% (v/v) glutaraldehyde in the same buffer for 2 hours at 2°C, the material was washed and left overnight at 2°C in corresponding buffer. Postfixation was done in 2% (v/v) OsO_4 (Stevens Metallurgical Corp., N.Y.) buffered by 0.1 M PBS, pH 6.9, for 6 hours at 2°C, after which the specimens were washed and left overnight in buffer at 2°C. The material was then dehydrated through a methanol series. For scanning electron microscopy, samples were then critical point dried using

liquid CO_2, sputter coated with gold and examined with a Cambridge Stereoscan 250T scanning electron microscope. For transmission electron microscopy, samples were further dehydrated into propylene oxide and infiltrated with Epon 812 (Polysciences Inc., Warrington, PA). Throughout fixation, dehydration and infiltration, the specimens were gently agitated via a mechanical rotator (Taab Laboratory Equipment Ltd., Berkshire, England) at 4 R.P.M. Silver sections were cut on a Reichert OMU3 ultramicrotome and stained in saturated methanolic uranyl acetate and lead citrate (Reynolds, 1963). Sections were examined with a Zeiss EM9S, a Zeiss EM10 or a Philips 400 electron microscopes.

Thick sections (0.75-1.0 µm) were also cut and dried onto glass slides. These sections were stained with 1% toluiding blue for 10 seconds over an alcohol lamp and examined with a Leitz Dialux 20 EB light microscope.

Morphometric analyses of light and electron micrographs of this material were carried out as described by Briarty (1980) with the following modification: only volumetric analyses were performed. A Weibel-type test system (Weibel, 1973) with a 21 line (7 x 3) array was employed to measure the cellular compartments at 1435X (light microscopy). Test points

lying over cytoplasm, cell wall, nuclei, central vacuole and chloroplasts were counted. Cytoplasmic compartments were measured at 6000X (electron microscopy) using a Weibel-type test system with an 84 line (14 x 6) array. Test points lying over chloroplasts, vesicles, nuclei, dictyosomes and mitochondria were counted. Volume density calculations were performed according to Weibel (1973).

Aplanospores were also collected and transferred to small petri dishes (12 per sample) containing chlorotetracycline (Sigma, St. Louis, MO) dissolved in culture medium to concentrations ranging from 10^{-3}M to 10^{-7}M. Control tests with aplanospores germinating in CTC-free culture medium were run parallel to the CTC experiments to determine the effect of different concentrations of CTC on germination.

For CTC-dependent Ca^{2+} localization, a freshly prepared solution of 10^{-4}M CTC was applied to material transferred from CTC-free cultures. CTC-treated material was then observed under a Leitz Dialux 20 EB compound microscope equipped with epifluorescence optics. All CTC fluorescence micrographs were taken 1 to 10 minutes after exposure to CTC. The possibility that CTC might fluoresce brightly even when not complexed with Ca^{2+} was checked by using the

Ca^{2+}-insensitive probe oxytetracycline [OTC] (Sigma, St. Louis, MO).

Morphometric analysis of the relative area occupied by CTC fluorescence was carried out by tracing micrographs enlarged to the same final magnification using a Hi Pad Digitizer (Houston Instruments, Austin, TX) and an IBM personal computer. The distribution and intensity of CTC fluorescence along the terminal 200 µm axis of the CTC-treated filaments was arbitrarily assessed from the same micrographs used to quantify the relative area occupied by CTC fluorescence.

Aplanospores were also subjected to the effects of three different antagonists of calcium in various concentrations: the chelator EGTA (10^{-3}M, 10^{-4}M, 10^{-5}M, 10^{-6}M), the calcium ionophore A23187 (10^{-4}M, 10^{-5}M, 10^{-6}M), and the calmodulin antagonist trifluoperazine [TFP] (10^{-4}M, 5 x 10^{-5}M, 2 x 10^{-5}M, 10^{-5}M). All chemicals were obtained from Sigma (St. Louis, MO). EGTA and TFP were added directly to the growth medium at the desired concentrations. The ionophore A23187 was first dissolved in DMSO before addition to the growth medium. A control with 1% DMSO added to the growth medium was run parallel to the experiments using the ionophore A23187. The growth of germinating filaments and CTC-dependent Ca^{2+} localization were then recorded over a 24 hr. period.

COLLECTION AND CULTURING

Morphologically the field collected plants of this variety of *Vaucheria longicaulis* are similar to those described by Blum (1971, 1972) for northern Washington. None of the British Columbian plants possess the extremely long antheridia characteristic of the species described from California (Hoppaugh, 1930).

Vaucheria longicaulis var. *macounii* is the most common brackish water species of *Vaucheria* in British Columbia and collections were made at a number of localities in the Strait of Georgia (Garbary and Fitch, 1984). At many sites *V. longicaulis* var. *macounii* was the only apparent species of *Vaucheria* in the field and this was confirmed through laboratory culture of several non-reproductive populations. However, it was often present intermingled with occasional filaments of *V. thuretii*. Plants form extensive mats in the high intertidal zone primarily on muddy substrate where they co-occur with *Salicornia* and other marsh phanerogams. Extensive collections were made from a population in North Vancouver, approximately 100 meters east of the north span of the Lion's Gate Bridge. In this particular location, healthy and extensive mats of *V. longicaulis* var. *macounii* have been found year round

throughout the four year duration of this study. At Blackie's Spit, an additional large population was found in the high intertidal zone on a sand beach.

When placed into culture, *V. longicaulis* var. *macounii* produced abundant aplanospores that have not been previously reported for this variety, although Taylor (1952) and Pecora (1979) report aplanospores in *V. longicaulis* from California and Louisiana, respectively. Taylor reports that aplanospores measure 225 µm in length and 90-120 µm in diameter comparing with 114-252 µm in length and 80-170 µm in diameter in the present material. Over 90% of aplanospores germinated within 48 hours of release and showed initial growth rates of 200-250 µm/h. The germlings often produced additional aplanospores and/or oogonia and antheridia within one week of germination.

APLANOSPOROGENESIS

Addition of fresh medium to field-collected cultures resulted in abundant aplanospore production (Fig. 1). Aplanosporogenesis is usually so prolific that nearly every filament produces an aplanospore.

Single aplanospores are differentiated terminally on vegetative filaments (Figs 1-5). However individual filaments often produce many aplanospores over a period of days.

The organization of the non-septate, coenocytic vegetative filament of V. longicaulis var. macounii is essentially the same as that reported by Ott and Brown (1974a) for eight other species of Vaucheria. The filament apices can be subdivided into three zones: the apical zone, sub-apical zone and zone of vacuolation. The same organization can be recognized at the beginning of aplanosporogenesis (Figs 8 and 21).

Ultrastructurally, both the apical zone and subapical zone contain many nuclei, mitochondria, chloroplasts and large numbers of vesicles containing fibrillar material (Figs 6 and 21). The fibrillar material-containing vesicles are particularly abundant at the apices of each filament. Another conspicuous feature is the presence of large numbers of dictyosomes always seen closely associated with endoplasmic reticulum elements and mitochondria. Microbody-like organelles are also seen in close association with these organelles (Fig. 7). A large central vacuole extends from the subapical zone. A single-layered cell wall surrounds the entire filament at the beginning of

aplanosporogenesis (Figs 8 and 11).

A gradual darkening and swelling of the vegetative filament tip indicates the onset of aplanosporogenesis (Figs 1 and 2). As the apical area expands, the central vacuole is displaced to a more subapical position (Figs 8 and 21). Autophagic digestion of materials of cytoplasmic origin (Fig. 9) and crystalline inclusions (Figs 8 and 10) are observed within the central vacuole. This single large central vacuole is eventually replaced by a network of smaller vacuoles which lend to the cytoplasm a highly reticulated morphology (c.f. Fig. 12 with Fig. 8). The mitochondria-ER-dictyosome complexes as well as the fibrillar material-containing vesicles remain abundant even though elongation of the vegetative filament has ceased at this time.

Some of the fibrillar material-containing vesicles release their contents by exocytosis adding new material to the existing cell wall. This process extends some distance down the vegetative filament and produces a second inner wall (Figs 16 and 17).

Septation of the aplanospore from the vegetative filament is initiated by the centripetal infurrowing of the newly formed inner wall at the base of the enlarged tip of the vegetative filament (Figs 3, 12 and 13). Cytoplasmic continuity remains intact until the

infurrowing inner wall severs the cytoplasm of the developing aplanospore from the cytoplasm of the remaining vegetative filament (Figs 14 and 15). At this stage, the original cell wall at the tip of the vegetative filament becomes the aplanosporangium wall (ASW) while the encircling inner wall becomes the aplanospore wall (AW) (Figs 16 and 19).

Both cell walls are composed of microfibrils arranged parallel to one another (Figs 16 and 17). The walls of the aplanospore and the aplanosporangium are usually of similar thickness (Fig. 16), but a thicker aplanospore wall is not uncommon (Fig. 17). Between the aplanospore and aplanosporangium walls there is a region of variable width (Fig. 17, *) containing fibrillar material comparable in morphology to that observed in the paramural space of the vegetative filament at the onset of aplanosporogenesis (Figs 6 and 11, *). This material is absent from the region separating both walls in more advanced stages of aplanospore development (Fig. 16) and hence its disintegration may be involved in the final isolation of the aplanospore within the aplanosporangium which occurs prior to its release (Fig. 20).

As the process of septation proceeds, leading to the formation of the aplanospore, a new central vacuole

develops concomitantly with the disappearance of the highly reticulated morphology of the cytoplasm (Figs 14 and 19; compare with Fig. 12). Nuclei are seen scattered throughout the aplanospore in no apparent pattern. Chloroplasts, numbered by the hundreds, are seen throughout the cytoplasm, although they are preferentially arranged against the plasma membrane of the aplanospore (Figs 6 and 15). This arrangement becomes more pronounced as the new central vacuole continues to expand within the maturing aplanospore (Figs 14 and 19). Large prominent pyrenoids are located centrally or terminally within the chloroplasts (Figs 6 and 18). Numerous dictyosomes consisting of 3-7 stacked cisternae are observed always in association with endoplasmic reticulum elements and mitochondria (Fig. 16); a condition that persists throughout aplanosporogenesis. A summary of the most important events leading to the individualization of the aplanospore within the aplanosporangium in *V. longicaulis* var. *macounii* is presented in Figure 21.

APLANOSPORE RELEASE AND GERMINATION

Emergence of mature aplanospores from aplanosporangia was monitored with the dissecting

microscope. An opening formed at the apical portion of the aplanosporangium wall through which the aplanospore emerged. Movement of the aplanospore out of the aplanosporangium was slow but continuous. Once free, it left behind an empty aplanosporangium wall casing (Fig. 24, small arrowhead) and slowly sunk to the bottom of the culture dish. Mature aplanospores measured 114-282 µm in length and 80-170 µm in diameter (Garbary and Fitch, 1984), while retaining the ellipsoid, obovate or oblong shape imparted during aplanosporogenesis (Figs 24 and 25, compare with Figs 5 and 20).

The study of the early phases of aplanospore germination can be divided into 3 main stages: Stage I = newly released aplanospore (Fig. 25); Stage II = onset of germination (Fig. 27); Stage III = approximately 1 hour after the initiation of germination (Fig. 28).

Sections through the center of a newly released aplanospore (stage I) reveal randomly scattered nuclei and hundreds of chloroplasts, many of which are peripherally arranged (Figs 25 and 29). Mitochondria-ER-dictyosome associations, with vesicles often seen blebbing off from the interspersed strand of the ER in transit to the cis-region of the dictyosomes, are also observed (Fig. 30). Fibrillar-material containing vesicles, produced by the trans-region of the

dictyosomes (Fig. 30, arrowheads), accumulate in the peripheral cytoplasm of the aplanospore in large quantities (Fig. 31, V). No discharge of vesicular material to the paramural space is seen at this stage. A cell wall of uniform thickness containing two morphologically distinct layers surrounds the newly released aplanospore. The thinner, amorphous outer wall layer contrasts with the thicker, microfibrillar one due to its higher electron density (Fig. 29).

Germination (stage II) is initiated by a protrusion of the cell wall at one or more locations along the surface of the aplanospore (Figs 26 and 27, arrowheads, Fig. 28). Up to four filaments have been seen arising from a single aplanospore (Fig. 22). Nearly all aplanospores germinate successfully within 48 hours of release. In the meantime, the underlying quiescent vegetative filament resumes its growth through the empty aplanosporangial case and may produce several more aplanospores. This leaves a node in the filament indicating where repeated aplanosporogenesis has occurred (Fig. 24, large arrowhead). *In situ* germination of aplanospores within aplanosporangia has also been observed when aplanospore release is delayed or fails to occur (Fig. 26).

The tip of the germinating protrusion (stages II

and III) is characterized by the presence of many mitochondria-ER-dictyosome complexes, densely-packed vesicles and a cell wall of irregular thickness (Fig. 31). Two distinct wall layers are still recognizable, however the outer wall layer shows signs of disruption (Fig. 31, c.f. with Fig. 29). Signs of exocytosis of vesicular contents to the paramural space and subsequent incorporation of this newly-released material into the inner layer of the aplanospore wall are also observed and account for the irregular thickness characteristic of these stages (Figs 32 and 33).

Figure 39 compares the volume densities of major cellular compartments during the three stages of aplanospore germination observed with light microscopy. The greatest overall changes observed in these compartments occur in the vacuole and chloroplasts. The volume of the vacuole increases during early germination from 23% (±4%) to 35% (±5%), and reaches 47% (±3%) of the total volume of the aplanospore by stage III. The volume density of this compartment keeps on increasing as germination proceeds until the aplanospore body is finally emptied of its contents (Fig. 23). Crystalline inclusions and large lipid bodies, absent since aplanosporogenesis, reappear concomitantly with the central vacuole's development and expansion (Figs 25 and

27). Meanwhile, the volume density of the chloroplast compartment decreases from 47% (±4%) in stage I to 40% (±5%) in stage II, and reaches a low value of 26% (±2%) in stage III. The volume density of the cell wall decreases by approximately one half through stages II and III of germination, while that of the nuclear fraction remains fairly constant at approximately 3% of the total aplanospore volume. The cytoplasmic fraction also remains relatively unchanged at 20-23% of the volume of the aplanospore during the early stages of germination.

Volume density changes in relation to total cytoplasmic volume density were also measured in several cellular compartments (Fig. 40). The volume density of the chloroplast compartment decreased during early germination from 49% (±6%) to 41% (±4%) and finally to 34% (±4%) of the cytoplasmic volume density at stage III (cf. with Fig. 39). The volume densities of the mitochondrial compartment increased from 5% (±2%) to 9% (±2%) and that of vesicles from 39% (±4%) to 52% (±5%) of the total cytoplasmic volume density. The large increase in the volume density of the vesicular compartment coincides with the accumulation in the peripheral cytoplasm of large numbers of fibrillar-material containing vesicles during stage I

and at an early phase of stage II (Fig. 31). Nuclear and dictyosomal compartments remain fairly constant at 2-4% of the total cytoplasmic volume density.

Non-preferentially oriented bundles of a few microtubules were observed in the cytoplasm of newly released (stage I) aplanospores (Fig. 34, arrowheads). Upon germination (stages II and III), the number of microtubules per bundle increases and the bundles become preferentially arranged parallel to the plasma membrane of the protruding filaments (Fig. 35, arrowheads). In addition, these larger microtubule bundles were often seen in close proximity to nuclei (Fig. 35) and chloroplasts.

In some aplanospores, large numbers of bacteria were seen within the cytoplasm, often in close proximity to the nucleus (Fig. 36). No apparent cytoplasmic damage was observed although small vacuoles containing bacteria in various stages of degradation were noted (Fig. 37). Bacteria were also occasionally seen penetrating the cell wall (Fig. 38). Interesting enough is the fact that these extensive signs of the occurrence of bacterial infection in aplanospores of *Vaucheria* have no apparent effect on the frequency or rate of germination of these reproductive cells.

Growth of germinating filaments of *V. longicaulis* var. *macounii* in various concentrations of CTC is shown in Fig. 41. Overall filament growth was greatest in the CTC-free control test and gradually decreased in CTC-treated material to 71% ±7% (10^{-7}M), 58% ±5% (10^{-6}M), 40% ±5% (10^{-5}M) and 31% ±5% (10^{-4}M) of the control over a 24 hour period, with no growth observed at 10^{-3}M CTC. Over periods of time of 6 hours or less, filament growth was very similar to the control in all but 10^{-3}M CTC. When 10^{-3}M CTC is added to germinating filaments, growth is immediately arrested and the filament tips tend to burst.

Figure 42 shows the growth rates of filaments treated in various concentrations of CTC during the first 6 hours of germination. During the first 2 hours, the growth rate of the material incubated in 10^{-4}M CTC varies from 42% to 52% of that observed in filaments treated with lower concentrations of CTC and represents only 39% (±6%) of that of the control. From 2 to 4 hours after germination, the growth rate of the material incubated in 10^{-4}M CTC remains virtually unchanged while the growth rates of all other CTC-tested material and the control steadily declines. From four to six hours after the initiation of germination, the decline in growth rate continues. In contrast, a recovery occurs

in 10^{-4}M CTC-treated material leading to growth rate values similar to that observed in the control by the end of this period. Stablized growth rates characterize subsequent post-germinative growth in all CTC-treated material and the control.

The absence of long term ill effects on the *Vaucheria* filaments from exposure to 10^{-4}M CTC can also be gathered from observations showing that this concentration of CTC does not affect the orientation or branching patterns of the germinating filaments when compared to that of the control material (cf. Fig. 45 with Fig. 46). Material incubated in 10^{-4}M CTC possesses the added advantage of showing higher fluorescence intensity than that observed with other concentrations (Fig. 51, compare with Fig. 50).

Bright field observations of germinating aplanospores reveal regions of lower optical density characteristic of the germination site(s) (Fig. 47). These coincide with the occurrence of localized CTC fluorescence (Fig. 48). In contrast, material treated with oxytetracycline (OTC), a Ca^{2+}-insensitive probe which is an analog of CTC (Wolniak *et al* 1980, Wise and Wolniak 1984), exhibits no fluorescence (Fig. 49).

A sharply-delimited region of CTC fluorescence is observed at the filament tip during the first 2 hours of

germination (Figs 50 and 52) and again from approximately 4 hours after germination and beyond (Fig. 53). A more diffuse pattern of CTC fluorescence, extending basipetally up to 200 um from the apex of the germinating filaments is observed between 2 and 4 hours after the initiation of germination (Fig. 54). A similar pattern of CTC fluorescence can also be detected in specimens of Vaucheria freshly collected from the field (Fig. 55). Transitional stages showing the transformation of well localized to more diffuse fluorescence are observed (Fig. 51).

The morphometric analysis of the relative area occupied by CTC fluorescence during germination and filament extension is shown in Figure 43. In Figure 44, the distribution and intensity of CTC fluorescence along the terminal 200 um of germinating filament axes are graphed. During the first 2 hours of germination, when the growth rate of control filaments is increasing (Fig. 42), CTC fluorescence occupies an area equivalent to 8% (±3%) of the terminal 200 um of the filament length (Fig. 43); almost all of which is localized at the tip (Fig. 44). From between 2 to 4 hours after the initiation of germination, when filament growth rates are rapidly slowing down and CTC fluorescence extends further away from the tip in a more diffuse manner (Figs

44 and 54), this area increases to 33% (±6%) of the total area of the growing filament (Fig. 43). In filaments germinating for 4 or more hours, CTC fluorescence is again reduced to 8.5% (±4%) of the total area of the growing filament (Fig. 43), with almost all of the fluorescence once more confined to the tip (Fig. 44). This pattern of tip-localized CTC fluorescence does not change significantly during subsequent post-germinative growth.

CALCIUM PERTURBATIONS

Untreated aplanospores and filaments used as control material for these experiments grew at rates ranging from 180 to 250 um/hr. These values are comparable to those previously reported (see also Garbary and Fitch, 1984). The morphological features and the sharply-delimited pattern of tip-localized Ca^{2+}, as visualized during the first 2 hours of germination with CTC fluorescence, also resembles that previously reported for Vaucheria (Figs 60 and 61, compare with Figs 47 and 52).

Figure 56 shows the effect of EGTA on both germination and filament growth in Vaucheria. The inhibitory effect of 10^{-3}M EGTA on filaments is

irreversible as recovery from growth inhibition by repeated washings and incubation in EGTA-free growth medium was unsuccessful. Over the 6 hour period of this experiment, the growth rates of newly germinated aplanospores gradually decreased in the EGTA-treated material to 92% ±8% (10^{-6}M), 78% ±6% (10^{-5}M) and 45% ±5% (10^{-4}M) of those observed in the control. No abnormal growth patterns or morphological alterations were observed as a result of the treatments with EGTA (Fig. 62 c.f. with Fig. 60). Filaments which had been incubated in 10^{-4}M EGTA and exposed to CTC two hours after the initiation of germination, resulted in a more diffuse overall pattern of fluorescence distribution. Nonetheless, most of the fluorescence is still concentrated near the tip; although, the fluorescence intensity is weaker than that of the control (Fig. 63 compare with Fig. 61).

Treatment with the ionophore A23187 resulted in varying degrees of growth inhibition. Growth rates decreased in the ionophore-treated material to 78% ±5% (10^{-6}M), 28% ±5% (10^{-5}M) and 8% ±4% (10^{-4}M) of the control (Fig. 57). Material incubated in growth medium with 1% DMSO grew at a rate virtually identical to that of the control (Fig. 57). Germinating filaments from aplanospores treated with A23187 are often broadened at

the base and of irregular diameter. The abnormalitites are more pronounced in material incubated in 10^{-4}M A23187, where swollen apices and bud-like protuberances corresponding to regions of low optical density are abundant (Fig. 64). In lower concentrations of A23187, the apical swelling and bud-like protrusions become less pronounced (Figs 66 and 67). Filaments grown in 1% DMSO display growth patterns and morphological features similar to those of the control (Fig. 68, compare with Fig. 60).

When material incubated in 10^{-4}M A23187 is stained with CTC, fluorescence is localized primarily in the abnormally swollen apices and bud-like protrusions observed along the germinating filaments (Fig. 65). The presence of fluorescence coincides with regions of lower optical density observed with bright-field microscopy (Fig. 64).

Aplanospores did not germinate, nor did filaments grow in any concentration of TFP tested (Fig. 58). Transferring TFP-treated material into normal medium did not lead to recovery from growth inhibition or germination, indicating the irreversibility of the effects of TFP on _Vaucheria_. Control specimens grew at rates similar to controls from the EGTA and A23187 experiments and continued to grow when subjected to the

same transfer procedure as the TFP-treated material. When TFP-treated material was stained with CTC, no fluorescence was observed (Fig. 69).

Figure 59 is a comparison of the growth rates graphed against the various concentrations of each of the three growth inhibitors used. TFP is clearly the most potent growth inhibitor followed by A23187 and EGTA, respectively. A23187 is more toxic than EGTA at each of the concentrations tested. The potency of A23187 is more pronounced than that for EGTA at 10^{-4}M. However, the toxicity of TFP is nearly the same as that of EGTA at 10^{-5}M and at 10^{-6}M.

APLANOSPOROGENESIS

Venkataraman (1961) and Chopra (1971) report zoospores as the most common method of asexual reproduction in Vaucheriaceae. Hibberd (1980) states that asexual reproduction in *Vaucheria* is exclusively by the production of synzoospores formed in zoosporangia. Neither Lee (1980) or Bold and Wynne (1985) acknowledge the presence of aplanospores in *Vaucheria* when describing this genus' modes of asexual reproduction in their textbooks; however, Smith (1950) and Christensen (1980) do. Zoospores are actually reported in fewer species of *Vaucheria* than aplanospores. Despite this descrepancy, no studies outside the taxonomic and ecologic realms have been conducted on aplanospores or aplanosporogenesis until now. In fact, ultrastructural studies of aplanosporogenesis or aplanospores in the phycological literature as a whole are virtually nonexistent.

The basic organization of the vegetative filament of *V. longicaulis* var. *macounii* and the initial stages of sporogenesis are similar to that reported by Ott and Brown (1974a, 1974b) for other species of *Vaucheria*. However, the mechanism of septation, leading to the formation of the spore, is strikingly different in

zoosporogenesis and aplanosporogenesis. Fritsch (1935) and Ott and Brown (1974b) describe a transverse bridge of colorless cytoplasm separating the zoosporangium from the vegetative cytoplasm prior to actual septation. Within a few minutes, these two separated cytoplasmic masses reapproach one another with each forming a membrane resulting in a septum that isolates the zoosporangium from the vegetative filament. The separation and reapproachment of cytoplasmic masses are not seen in aplanosporogenesis. Rather, observation of septation via the centripetal infurrowing of the inner wall at the base of the enlarged tip of reproductive filaments occurred. This infurrowing mechanism resembles cleavage furrows described in spermatogenesis of _Vaucheria_ (Ott and Brown, 1978) and in cytokinesis, tetrasporogenesis and spermatogenesis of red algae (Scott 1983, Pueschul 1979, Vesk and Borowitzka 1984, Cole and Sheath 1980). This constricting inner wall isolates the mature aplanospore from the vegetative filament, while becoming part of the cell wall of the maturing aplanospore. Taylor (1952) reported that there was no wall present in aplanospores from _V. longicaulis_ collected in California; a situation similar to the one observed in zoospores of _V. fontinalis_ (Christensen) prior to germination (Ott and Brown, 1975). However,

the presence of a complete wall around the aplanospore prior to release and settlement has been reported in the genus Vaucheria by Fritsch (1935) and Rieth (1980) and is further confirmed in the present study. Previously reported in vegetative filaments of V. sessilis (Vauch.) DeCandolle (Greenwood, 1959), V. fontinalis (L.) Christensen and V. dilwynii (Weber et Mohr) C. A. Agardh (Ott and Brown, 1974a), the mitochondrion-dictyosome association is also present in V. longicaulis var. macounii. This association persists throughout aplanosporogenesis and contrasts with zoosporogenesis where the mitochondria-dictyosomal associations gradually disappear (except in the apex) until germination of the zoospore occurs (Ott and Brown, 1974b, 1975). The band of endoplasmic reticulum and vesicles seen interspersed between the mitochondrion and dictyosomes appear in all Vaucheria species studied to date. A similar mitochondria-ER-dictyosomal association has also been reported in the Oomycete Saprolegnia (Heath and Greenwood, 1971). The association of a mitochondrion adjacent to a dictyosome may be functionally important in a coenocyte like Vaucheria where vigorous cytoplasmic streaming might otherwise cause these organelles to become separated by considerable distances. Yet, other coenocytes lack this

type of association (Penicillus, Turner and Friedman 1974, Dichotomosiphon, Moestrup and Hoffman 1973, Pseudodichotomosiphon, Hori et al. 1979, Bryopsis, Burr and West 1970) and still remain functional. Heath and Greenwood (1971) suggested that this association may facilitate efficient energy transfer between the organelles. The coupling of an energy production site (the mitochondrion) with energy utilization sites (dictyosomes and ER) could then be functionally significant for the intensive secretory activity of dictyosomes leading to the formation of the aplanospore wall as suggested for tetrasporogenesis in certain red algae (Pueschul, 1979) . However, the actual role and forces retaining this association remain enigmatic.

The formation of a new central vacuole within the developing aplanospore prior to release from the aplanosporangium was not seen in zoosporogenesis (Ott and Brown, 1974b). The coalescence of many small vacuoles into a new central vacuole may build turgor pressure within the aplanospore so that it can germinate immediately upon release through localized turgor-driven cell wall expansion (Fitch and Oliveira, 1986b). Pyrenoids were reported lacking in Vaucheria filaments (Fritsch 1935, Ott and Brown 1974a) and zoospores (Greenwood 1959, Ott and Brown 1974b,

1975). This is in contrast with our findings and those of Marchant (1972) in aplanospores of V. woroniniana. In zoosporogenesis, nuclei with associated centrioles converge on the plasma membrane leading to the formation of flagellar pools (Ott and Brown, 1974b). This contrasts with aplanosporogenesis where nuclei remain scattered throughout the cytoplasm and neither flagellar initiation or assembly are observed.

Table I contrasts aplanosporogenesis in V. longicaulis var. macounii with zoosporogenesis in V. fontinalis and reveals that aplanospores may be more than simply "ontogenetically potential zoospores" (Bold and Wynne, 1985). Christensen's (1980) description of aplanospores in Vaucheria as "...reproductive cells that start their development in the same way as zoospores but then assume an approximately spherical shape and surround themselves with walls without having formed flagella" more accurately describes the aplanospores in V. longicaulis var. macounii. Although some ultrastructural and developmental similarities are seen in aplanosporogenesis and zoosporogenesis, significant differences exist between these two processes as well. Such differences warrant further study of the process of aplanosporogenesis in the Tribophyceae and in all aplanospore-producing algae in general.

TABLE I

APLANOSPOROGENESIS vs ZOOSPOROGENESIS

ULTRUSTRUCTURAL FEATURE	APLANOSPOROGENESIS*	ZOOSPOROGENESIS**
Cell Wall	Present	Absent
Mitochondria-ER-Dictyosome	Present	Gradually disappears (except at apex)
Fibrillar material-containing vesicles	Present in large numbers; contain wall material	Gradually disappear
Central Vacuole	Vacuole displaced, transformed into reticulate pattern, reappears	Absent
Chloroplasts	Many peripherally arranged, pyrenoid present	Randomly scattered, Pyrenoid absent
Nuclei	Always randomly scattered	Parietally positioned in late zoosporogenesis
Flagella	Absent	Present

* *V. longicaulis* var. *macounii* (Fitch and Oliveira, 1986a)
** *V. fontinalis* (Ott and Brown, 1974b)

Taylor (1952) reported that dissolution of the distal aplanosporangium wall leads to liberation of aplanospores in V. longicaulis. Enzymatic degradation of the zoosporangium wall was reported during zoospore release in V. fontinalis (Ott and Brown, 1975). In our material, however, polysaccharide-wall degrading enzymes would tend to break down (in addition to the aplanosporangium wall) the already secreted aplanospore wall. This would affect the structural integrity of the aplanospore and hence it is unlikely to occur.

We have observed an accumulation of mucilaginous-like material between the mature aplanospore and the aplanosporangium wall of V. longicaulis var. macounii (Fitch and Oliveira, 1986a). Swelling of the mucilaginous material surrounding the aplanospore could then rupture the distal end of the aplanosporangium and facilitate aplanospore release. In addition, the coalescence of many small vacuoles into the new central vacuole, observed during aplanosporogenesis (Fitch and Oliveira, 1986a), may help build up sufficient turgor pressure within the aplanospore to aid in bursting open the aplanosporangium. These observations are in agreement with those of Fritsch (1935) and Venkataraman (1961)

suggesting that osmotic pressure build-up within the intact aplanosporangium leads to the apical rupture followed by contraction of the aplanosporangium wall and the subsequent release of the aplanospore.

Besides its involvement in aplanospore release, turgor pressure has also been cited as the moving force behind plant (Pickett-Heaps, 1977, Burns *et al*, 1982) and fungal (Buller, 1958) cell elongation. In *V. longicaulis* var. *macounii*, the coalescence of small vacuoles with the central vacuole during aplanosporogenesis (Fitch and Oliveira, 1986a) and the rapid volume expansion of the central vacuole during the early stages of aplanospore germination support this proposal.

The cell wall at the tip of the germinating filament must maintain its structural integrity while yielding to the turgor-driven force of the rapidly expanding central vacuole. The presence of a non-uniform cell wall at the germination site(s) on the aplanospore together with the morphometric data showing a decrease in the volume density of the cell wall compartment during the early stages of germination, reflects the dual role that the cell wall must perform. Germination and tip growth can, therefore, be considered a dynamic balance between wall lysis to yield to turgor

pressure development, as evidenced by disruption of the outer wall layer, and new wall synthesis to maintain filament integrity, as evidenced by incorporation of released materials to the inner wall layer (Garraway and Evans, 1984).

Heath and Greenwood (1971), Ott and Brown (1974a) and Aghajanian (1979) have postulated that a close association between mitochondria and dictyosomes facilitates efficient energy transfer within the cell. The persistence of this association, first observed in Vaucheria by Ott and Brown (1974a, 1974b, 1975) and confirmed by our work on aplanosporogenesis (Fitch and Oliveira, 1986a), may be necessary to support the rapid growth rate (approx. 250 um/hr.) of the filaments during the early stages of germination. Although dictyosomal volume density does not increase during germination, an increase in dictyosomal efficiency is suggested by both an accumulation of vesicles at the tip of the germinating filaments (Fig. 10) and an increase in vesicle volume density that remains significantly high during the active periods of stages II and III and in subsequent germination (Fig. 19). These observations together with the increase observed in the mitochondrial volume density during stages II and III indicate a high metabolic rate for the synthesis and export of materials

to the inner layer of the cell wall by the mitochondria-ER-dictyosomal complexes (Fig. 9).

During stage I, small bundles of microtubules were seen scattered in the cytoplasm. This is in contrast with germination (stages II and III) and subsequent filament extension in which microtubule bundles appear more numerous and show preferential arrangement near the plasma membrane. Increases in microtubule numbers have been noted in the germinating spores of the moss Funaria (Schnepf et al., 1982), in pollen tubes of Lilium (Reiss and Herth, 1979a), in the tips of actively growing fungal hyphae (Howard and Aist, 1980) and in budding yeast cells (Garraway and Evans, 1984). Increases in microtubule number accompanied by their association with nuclei and chloroplasts were reported by Ott and Brown (1974a) in Vaucheria litorea and Schnepf et al (1982) in the moss Funaria hygrometrica. These observations seem to indicate that directional movement of organelles by microtubules and/or microfilaments is essential in establishing the polarity of germination and in orchestrating the development of reproductive structures in Vaucheria.

Endosymbiotic bacteria have previously been reported in three species of Vaucheria (Ott, 1979). This author believes this may be a mutualistic

relationship. This interpretation is particularly attractive in light of current results showing the occurrence of a significant decrease in the volume density of the chloroplast compartment during germination. This could conceivably be translated into lower photosynthetic capacity and the need to supplement the high energetic demands imposed on the germinating aplanospore by other means. Bacterial digestion within vacuoles may then be important in supplying the aplanospore with some nutrients. The fact that there is no apparent effect on the rate of aplanospore germination due to large numbers of intact bacteria lying in the cytoplasm close to nuclei lends support to this interpretation. More work is required, however, on this subject since the observation in our material of some bacteria within digestive vacuoles may be part of a defensive response to bacterial infection by the aplanospores.

CALCIUM LOCALIZATION WITH CHLOROTETRACYCLINE

Various concentrations of CTC have been used to observe the distribution of calcium in living plant and animal cells (Wolniak *et al* 1980, Meindl 1982, Kiermayer and Meindl 1984, Kauss and Rausch 1984,

Glowacka *et al* 1985), with a concentration of 10^{-4}M being the most frequently utilized (Chandler and Williams 1978a,b, Reiss and Herth 1978, 1979b, 1982, 1985, Reiss *et al* 1983, Reiss *et al* 1985). Caswell (1979) suggests that CTC should not be used above a concentration of 10^{-4}M since higher levels may disrupt the response being monitored. However, the suitability of this CTC concentration must be tested in each case since cells from different organisms display varying degrees of sensitivity to CTC as an antibiotic (Baloun and Hudak 1979, Reiss and Herth 1979b, Saunders and Hepler 1981). For example, 10^{-4}M CTC is reported to have no deleterious effects on the fungus *Achlya* and the alga *Acetabularia* (Reiss and Herth, 1979b), the liverwort *Riella* (Grotha, 1983), and the moss *Funaria* (Saunders and Hepler, 1981). However, *Lepidium* (cress) root hairs show a tendency to burst when treated with 10^{-4}M CTC (Reiss and Herth, 1979b). Prolonged treatment with 10^{-4}M CTC also causes disoriented growth, abnormal wall thickenings and apical swelling in *Lilium* pollen tubes after 30 minutes of exposure and eventually results in complete cessation of growth after 2 hours of treatment (Reiss and Herth, 1982). In the desmid *Micrasterias*, growth is stopped within minutes, the wall is abnormally thickened and death occurs after 6 to 8 hours in 10^{-4}M

CTC (Hausser and Herth, 1983).

In Vaucheria, total filament length is diminished but growth is not stopped in 10^{-4}M CTC, while the growth rate shows a significant recovery between 4 to 6 hours after initiation of germination prior to becoming stabilized. In addition, the morphology and orientation of Vaucheria filaments remain unaffected by this treatment. Concentrations of CTC greater than 10^{-4}M show brighter fluorescence. However, neither germination nor growth occurred at these levels, while the fluorescence intensity produced by using lower concentrations of CTC becomes reduced. Since all observations were made within 1 to 10 minutes of CTC application, a time when the growth rate of treated filaments is similar to that of the control, the 10^{-4}M CTC concentration is the best compromise between bright fluorescence and healthy metabolic activity in Vaucheria.

Calcium accumulations at the apices of Lilium pollen tubes have been demonstrated using autoradiography (Jaffe et al, 1975), a proton-microprobe (Reiss et al, 1983) and CTC fluorescence (Reiss and Herth, 1978, 1982). Jaffe et al (1975) found that the accumulation of Ca^{2+} was 2 to 4 times higher at the apex than in the bulk of the pollen tubes where Ca^{2+} accumulations did not occur. Reiss et al (1983)

reported that in Lilium pollen tubes, the maximum calcium content lies within the terminal 7 um; a region rich in endoplasmic reticulum, mitochondria and golgi-derived vesicles, organelles known to participate in the storage of Ca^{2+} ions (Herth 1978, Picton and Steer 1982, Reiss et al 1983). Since CTC is known to accumulate and bind Ca^{2+} to cellular membranes (Caswell 1979, Reiss and Herth 1982), those results concur with our findings that, in Vaucheria, the maximum fluorescence, and hence Ca^{2+} concentration, lies within the tip of the germinating filament. This region is also rich in organelles such as vesicles and mitochondria (Fitch and Oliveira, 1986b) known to be capable of storing cellular calcium.

The more diffuse distribution of CTC fluorescence seen in Vaucheria filaments between 2 and 4 hours after germination may indicate a release of Ca^{2+} from intracellular storage and/or an influx of Ca^{2+} from the extracellular compartment into the cytoplasm. Influx of Ca^{2+} would be required for the maintenance of an area of high intensity fluorescence at the tip of the filaments, while release of Ca^{2+} from intracellular storage could mainly account for the progressive increase in the area occupied by CTC fluorescence. A widespread increase in Ca^{2+} distribution, due to a rise in free cytoplasmic

Ca^{2+}, leads to growth inhibition in *Lilium* pollen tubes (Herth 1978, Reiss and Herth 1979a,b, Picton and Steer 1982). The same phenomenon may then be responsible for the reduced growth rate observed between 2 and 4 hours after the initiation of germination in our material. From approximately 4 hours after germination and beyond, CTC fluorescence returns to a tip-localized pattern suggesting that excess free cytoplasmic Ca^{2+} may have been resequestered into known sub-cytoplasmic Ca^{2+} pools (Reiss and Herth 1978, Wolniak *et al* 1980, Saunders and Hepler 1981, Wise and Wolniak 1984, Kauss and Rausch 1984).

In *Funaria*, bud formation is triggered by the accumulation at the growing tip of Ca^{2+} channels. These promote Ca^{2+} influx leading to localized microdomains of increased Ca^{2+} concentration (Saunders, 1986). There is evidence in *Acetabularia*, and it has been suggested in *Sphacelaria*, that the establishment of growth regions also coincides with external acidification of the cell wall due to the action of proton pumps (Burns *et al* 1984, Goodwin and Trainor 1985). Increased external proton concentration is known to cause displacement of Ca^{2+} ions from the cell wall resulting in locally increased Ca^{2+} influx across the plasma membrane (Goodwin and Trainor, 1985). Such a transient increase

in cellular calcium has been suggested to result in exocytosis and insertion into the surface membrane of H^+-ATPase transport systems (van Adelsberg and Al-Awqati, 1986). Further acidification of the cell wall could then tilt the balance of Ca^{2+} distribution towards a temporary accumulation of Ca^{2+} in the peripheral cytoplasm. The localized CTC fluorescence identifying the germinating regions of aplanospores and the filament tips of Vaucheria may then reflect the existence of similar mechanisms leading to the displacement of Ca^{2+} ions. Indeed, localized ion currents across the plasma membrane have previously been reported in Vaucheria sessilis and other tip-growing cells (Quatrano 1978, Weisenseel and Kicherer 1981). These contribute to the accumulation of golgi-derived vesicles at the growth pole(s) and promote their fusion with the cell membrane (Weisenseel and Kicherer, 1981), resulting in oriented exocytosis of polysaccharide-storing vesicles necessary for apical wall expansion (Herth 1978, Reiss and Herth 1978, 1979a, 1979b, 1982, Weisenseel and Kicherer 1981). The accumulation and subsequent exocytosis of vesicles at the tip of Vaucheria filaments (Ott and Brown 1974, Kataoka 1982, Fitch and Oliveira 1986a,b), concomitant with a well-defined tip-localized CTC fluorescence

observed during periods of rapid increase in growth rate, suggests that differences in electrical potential due, at least partially, to Ca^{2+} ion redistribution, are also responsible for the establishment of polarized germination and growth in Vaucheria.

Calcium is known to be involved in the regulation of the viscoelasticity of the gel-like cytoplasm rich in cytoskeletal elements found adjacent to the plasma membrane (Goodwin and Trainor, 1985). Localized high levels of Ca^{2+} causes depolymerization of microtubules and decreases the viscosity of the cytoplasm (Picton and Steer 1982, Goodwin and Trainor 1985). This loosening of cytoplasmic structure in conjunction with vacuole-derived turgor pressure due to the rapid expansion of the central vacuole of germinating filaments (Fitch and Oliveira, 1986b) will then facilitate growth. Concomitantly, cytoplasmic integrity at the tip of growing filaments is maintained by a network of microfilaments which are stabilized by high levels of Ca^{2+} ions (Picton and Steer, 1982). Although microfilaments have not been documented in our material, due possibly to their disruption by glutaraldehyde fixation, their presence has previously been reported in Vaucheria (Ott and Brown, 1974). This dual opposing actions of Ca^{2+} on different components

of the cytoskeletal apparatus may then play an important role in regulating the balance between integrity and flexibility that must occur at the tip(s) of the aplanospore and germinating filaments for growth to take place without bursting the cell wall (Fitch and Oliveira, 1986b).

CALCIUM PERTURBATIONS

Besides direct observation of the intracellular localization of Ca^{2+} by CTC, another way to obtain information on the role of Ca^{2+} in these phenomena is to use compounds which alter the intracellular Ca^{2+} gradients and availability, and to observe whether or not metabolic parameters, such as growth rates, are changed as a consequence of alterations in the distribution of Ca^{2+} (Kauss and Rausch, 1984). For this purpose, we used three growth inhibitors known to alter the availability of Ca^{2+} to the cell: the chelator EGTA, the ionophore A23187 and the phenothiazine-type calmodulin antagonist TFP.

EGTA selectively chelates Ca^{2+} external to the plasmalemma yet is unable to penetrate biological membranes (Blinks _et al_ 1982, Al-Khazzar _et al_ 1984, van Adelsberg and Al-Awqati 1986, Volberg _et al_ 1986). EGTA

concentrations of 10^{-5}M or greater have been shown to inhibit growth in the desmid Micrasterias (Lehtonen, 1984), prevent hyphal extension in Achlya bisexualis (Harold and Harold, 1986), inhibit protoplast fusion in Daucus carota (Grimes and Boss, 1985), prevent Ca^{2+} uptake by human erythrocytes (Foder et al, 1984) and delay the onset of anaphase in Haemanthus endosperm cells (Wise and Wolniak, 1984). Results obtained in this work show that EGTA concentrations of less than 10^{-4}M reduces growth rates, while EGTA concentrations greater than 10^{-4}M completely inhibit both germination and growth. The data suggest that the availability of extracellular Ca^{2+} is essential to aplanospore germination and growth in Vaucheria.

EGTA has also been found to reduce or quench CTC fluorescence in the rhizoids of the fern Onoclea sensibilis (Miller et al, 1983), in gemmalings of the liverwort Riella helicophylla (Grotha, 1983), in Haemanthus endosperm cells (Wolniak et al, 1980) and in pollen tubes of various plants (Polito, 1985). Present observations in which the intensity of the CTC fluorescence is diminished in EGTA-treated material provides evidence that much of the CTC fluorescence in untreated cells is due to the tip-localized influx of Ca^{2+}. Therefore, a decrease in CTC fluorescence in

EGTA-treated cells seems to indicate a reduction in Ca^{2+} influx.

EGTA-treated material also showed a more diffuse distribution of CTC fluorescence resembling that observed in untreated specimens between two to four hours after the initiation of germination. This occurs concomitantly with a reduction in growth rates suggesting an alteration in the influx of Ca^{2+} into the cytoplasm and/or the release of Ca^{2+} from intracellular storage as well. This temporary alteration in the distribution and availability of cellular Ca^{2+} indicates disruptions in normal Ca^{2+} gradients, hence of associated ionic currents. These observations concur then with those of Wiesenseel and Kicherer (1981) showing that the growth rate of Vaucheria is dependent upon the influx of specific extracellular ions, possibly Ca^{2+} ions, which produces the transmembrane ionic current necessary for maintaining tip-oriented exocytosis which is known to play a major role in aplanospore germination and growth (Fitch and Oliveira, 1986b).

The ionophore A23187 is known to inhibit growth in Lilium pollen tubes (Herth 1978, Reiss and Herth 1979a) and in the unicellular alga Micrasterias (Lehtonen, 1984). Abnormal growth and branching patterns due to

A23187 are reported in *Lilium* pollen tubes (Herth 1978, Reiss and Herth 1979a), in the water mold *Achlya bisexualis* (Harold and Harold, 1986), in *Micrasterias* (Lehtonen, 1984) and in the caulonema of the moss *Funaria* (Sievers and Schnepf, 1981). In *Vaucheria*, this compound lowers the growth rate of the germinating filaments and stops growth when applied at concentrations of 10^{-4}M or above. The treatment also creates morphological abnormalities in the growing filaments.

The ionophore A23187 is known to release Ca^{2+} from internal storage, such as mitochondria and endoplasmic reticulum (Chandler and Williams 1978b, Herth 1978, Reiss and Herth 1979a, Al-Khazzar *et al* 1984, Grimes and Boss 1985, Harold and Harold 1986) and/or increase Ca^{2+} flux into the cell (Herth 1978, Weisenseel and Kicherer 1981, Al Khazzar *et al* 1984, Foder *et al* 1984, Irving *et al* 1984, Kauss and Rausch 1984, Lehtonen 1984, Skibsted *et al* 1984, Grimes and Boss 1985). Therefore, when A23187 is added to cultures, presumably the extra- and intracellular Ca^{2+} become equilibrated, thus significantly raising intracellular Ca^{2+} concentrations.

Herth (1978) showed that in *Lilium* pollen tubes, depolarized growth is due to the delocalization of Ca^{2+} from apical growth sites. Lehtonen (1984) also showed

that the disruption of Ca^{2+} influx through the plasma membrane in Micrasterias by A23187 leads to disoriented growth due to delocalized exocytosis of dictyosome-derived vesicles, containing wall precursors, which results in morphological abnormalities. These observations concur with present findings that in Vaucheria, morphological abnormalities produced by A23187 treatments appear as bud-like protrusions with most of the CTC fluorescence localized in them (Fig. 65). Morphological abnormalities could also result from ionophore-dependent variations in Ca^{2+} gradients and their implications for the stability of the cytoskeleton. However, it has been found that microtubule integrity is unaffected *in vivo* by the presence of A23187 (Lonergan, 1984). On the other hand, it has been reported that A23187 can disrupt oxidative phosphorylation (Reed and Lardy, 1972). The calcium ionophore A23187 was also said to primarily affect wall formation in pollen tubes (Reiss and Herth, 1979a) and the caulonema of Funaria (Schmeidel and Schnepf, 1980). Therefore, whether these phenomena are directly induced by Ca^{2+}-related perturbations of cytoskeletal proteins and exocytosis or other causes cannot be determined at present.

To ascertain the importance of these various

phenomena and the role Ca^{2+} plays in them, it would be of interest to lower the intracellular Ca^{2+} level. To perform this type of experiment *in vivo*, it would be necessary to reduce the Ca^{2+} concentration in the growth medium to a value below that of free intracellular Ca^{2+} and then lower its intracellular concentration by introducing an ionophore that equilibrates extra- and intracellular Ca^{2+}. The problem is that the simple action of lowering Ca^{2+} concentrations in the growth medium, to a value most probably still above that of free intracellular Ca^{2+}, results in the complete cessation of growth. Another possibility is to determine whether or not calmodulin-regulated phenomena, such as cytoskeletal stability, is involved in the complex process of aplanospore germination.

Calmodulin is known to participate in the calcium regulation of protein phosphorylation, of some enzymatic activities, calcium flux across cell membranes, microtubule assembly and cell shape maintenance (Skibsted *et al* 1984, Grimes and Boss 1985, Marmé 1985, Smedley and Stanisstreet 1985). Phenothiazine compounds, such as TFP, are known to bind to the calcium-activated form of calmodulin; hence acting as calmodulin antagonists (Bar-Sagi and Proves 1983, Horwitz *et al* 1981). TFP is reported to inhibit wound

healing in *Xenopus* embryos (Smedley and Stanisstreet, 1985), inhibit growth in pollen tubes of *Tradescantia virginiana* (Picton and Steer, 1985), *Pyrus communis*, *Juglans regia* and *Prunus dulcis* (Polito, 1985), and to inhibit fusion of *Daucus carota* protoplasts (Grimes and Boss, 1985). In human erythrocytes, TFP prevents the transport of Ca^{2+} ions through Ca^{2+} channels in the plasma membrane by binding to the transport enzyme and to calmodulin itself (Foder *et al* 1984, Skibsted *et al* 1984). TFP is also known to inhibit Ca^{2+} influx in roots of *Lepidium sativum* (Buckhout, 1984) and other plants (Grimes and Boss 1985, Picton and Steer 1985, Polito 1985). Therefore, calmodulin plays an important role in governing intracellular Ca^{2+} concentrations (Picton and Steer, 1982).

Since neither germination nor growth occurred in *Vaucheria* in the presence of TFP, it seems Ca^{2+} influx may have been inhibited by the treatment. The absence of CTC fluorescence in TFP-treated material shows that the treatment possibly disturbs the storage of intracellular Ca^{2+} as well. This is not surprising given the fact that the control of cytoplasmic Ca^{2+} in plant as well as in animal cells is, at least partially, dependent on the calmodulin regulated accumulation of Ca^{2+} in cellular organelles such as mitochondria and

endoplasmic reticulum (Marme, 1985).

Schliwa *et al* (1981) reported that calmodulin inhibitors can completely inhibit Ca^{2+}-induced microtubule depolymerization in lysed animal cells. These findings together with the available evidence suggesting a role for Ca^{2+}-calmodulin regulation of microtubule depolymerization *in vivo* (Keith *et al* 1983, Schliwa *et al* 1981) could explain growth cessation in TFP-treated *Vaucheria* due to interference with the preferential arrangement of cytoplasmic microtubules observed during aplanospore germination (Fitch and Oliveira, 1986b).

The possibility that calmodulin may be involved in the regulation of microtubule-microtubule and possibly microtubule-organelle interactions rather than microtubule stability has also been advanced (De Mey *et al*, 1980). Disruptions in these systems could lead to an impairment in the transport of Golgi-derived vesicles containing cell wall precursors to the cell surface (Fitch and Oliveira, 1986b). Papahadjopoulos (1978) proposed that calcium participates in the regulation of the physical structure of the membrane bilayer and thus controls the fusion of membranes. This would also lead to the disruption of the exocytosis of materials necessary for cell wall expansion (Fitch and Oliveira,

1986b) and hence to growth cessation in TFP-treated material. TFP-induced disturbance on Ca^{2+} gradients can, therefore, affect in a variety of ways the organization of the apical cytoplasm of *Vaucheria* filaments; thus stopping growth and germination.

The implications of the ultrastructural and ontogenetic differences between aplanosporogenesis (aplanospores) and zoosporogenesis (zoospores) should not be overlooked. The presence of a complete cell wall and central vacuole and the maintenance of a wall-producing apparatus throughout aplanosporogenesis (Fitch and Oliveira, 1986a) appear to prepare the aplanospore for immediate germination and rapid growth upon release. These ultrastructural and physiological adaptations make the aplanospore a suitable vector for asexual reproductive success in some *Vaucheria* species. Judging by the extensive and persistent growth of *V. longicaulis* var. *macounii* in coastal salt marshes of the Pacific Northwest, dispersal and growth via aplanospores appears critical to the continued presence and expansion of this alga.

The combination of increasing turgor pressure (Fitch and Oliveira, 1986b), acidification and weakening of the apical cell wall (Burns *et al*, 1984), Ca^{2+} redistribution and its effects on the stabilization of the cytoskeletal network (Picton and Steer, 1982) and exocytosis of vesicles at the growth sites (Jaffe *et al* 1975, Herth 1978, Picton and Steer 1982, van Adelsberg and Al-Awqait 1986) are important aspects of the complex mechanism controlling polarized germination and growth

in Vaucheria aplanospores. Further studies are required to confirm the light microscopic observations of Ca^{2+} localization in the germinating protrusions and filament tips of Vaucheria. This work should be extended to include other known Ca^{2+} antagonists in order to get a better understanding of the roles of extra- and intracellular Ca^{2+} in these phenomena.

The use of microtubule and microfilament inhibitors, such as colchicine and cytochalasin B, and fluorescence microscopic studies using monoclonal antibodies to localize cytoskeletal elements in conjunction with CTC-dependent localization of Ca^{2+} should help elucidate the role of the cytoskeleton and the influence of Ca^{2+} in the germination and growth of Vaucheria aplanospores. Of particular importance would be measuring actual variations in cellular Ca^{2+} concentrations by the use of fluorescence compounds such as Quin 2. Cytochemical localization and X-ray microanalysis may also prove valuable techniques in further understanding the role of Ca^{2+} in germination and tip-oriented growth.

KEY FOR FIGURES

A = aplanospore

AV = autophagic vesicle

AW = aplanospore wall

ASW = aplanosporangium wall

B = bacterium

Ch = chloroplast

Cry = crystalline inclusion

CW = cell wall

D = dictyosome

DV = digestive vacuole

ER = endoplasmic reticulum

L = lipid body

M = mitochondrion

Mb = microbody-like organelle

N = nucleus

Nu = nucleolus

P = pyrenoid

PM = plasma membrane

RER = rough endoplasmic reticulum

Th = thylakoid

V = fibrillar material-containing vesicle

Vac = vacuole

VF = vegetative filament

* = paramural fibrillar material

Fig. 1. Aplanosporogenesis in *V. longicaulis* var. *macounii* induced by the addition of fresh medium.

Fig. 2. The initiation of aplanosporogenesis is marked by swelling at the tip of the vegetative filament.

Fig. 3. Initiation of septation of the aplanospore by the infurrowing inner wall (arrowheads).

Fig. 4. Completion of septation leading to the individualization of an aplanospore from the vegetative filament (arrowhead).

Fig. 5. Mature aplanospore within the aplanosporangium prior to its release. Note the aplanosporangial wall (arrowhead).

Fig. 6. Detail of the organelles seen in the tip of a vegetative filament during aplanosporogenesis.

Fig. 7. Detail of a mitochondrion-endoplasmic reticulum-dictoysome association. Also shown in close relationship to these organelles is a microbody-like organelle.

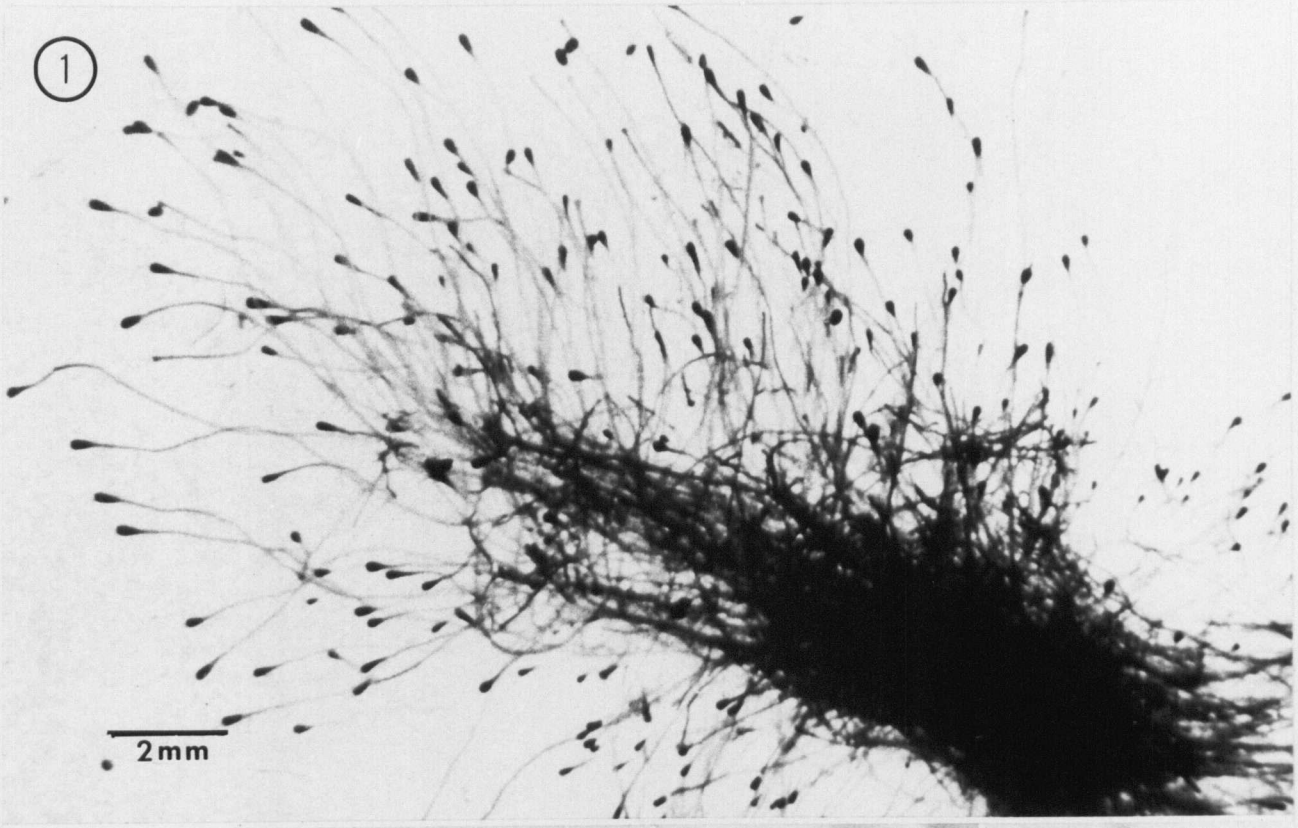
1
2mm

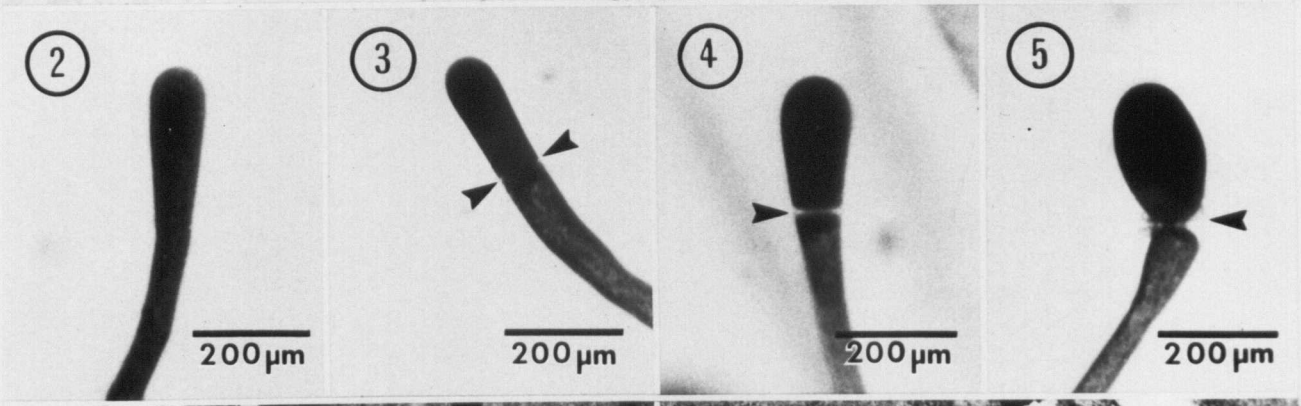
2
200µm
3
200µm
4
200µm
5
200µm

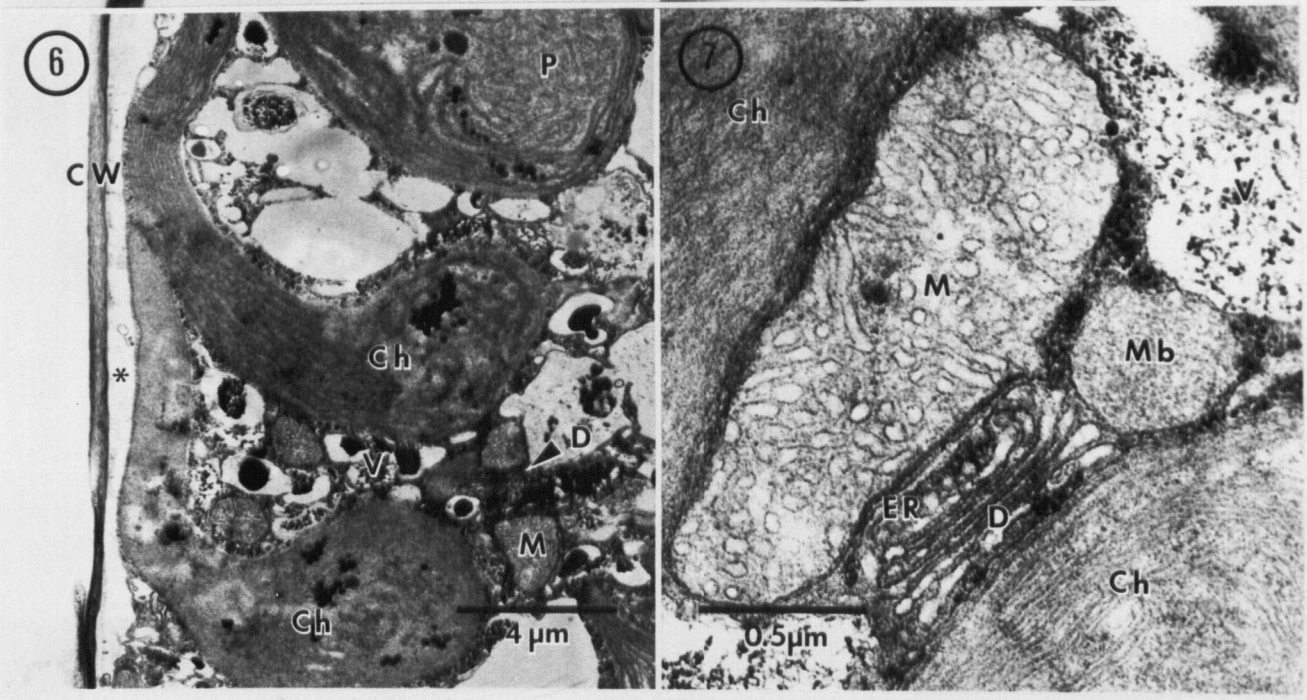
6
P
CW
Ch
*
V
D
M
Ch
4 µm
7
Ch
V
M
Mb
ER
D
Ch
0.5µm

Fig. 8. Aplanosporogenesis; early stage. Note the subapical position of the central vacuole. Crystalline inclusions are observed within the vacuole. Densely packed chloroplasts occupy the apical cytoplasm.

Fig. 9. Autophagic digestion of cytoplasmic remnants within the vacuole.

Fig. 10. Detail of a crystalline inclusion observed within the vacuole (Fig. 8, cry).

Fig. 11. Accumulation of fibrillar material in the paramural space (*) of the tip of the vegetative filament at an early stage of aplanosporogenesis (see Fig. 6 also). Note the single cell wall.

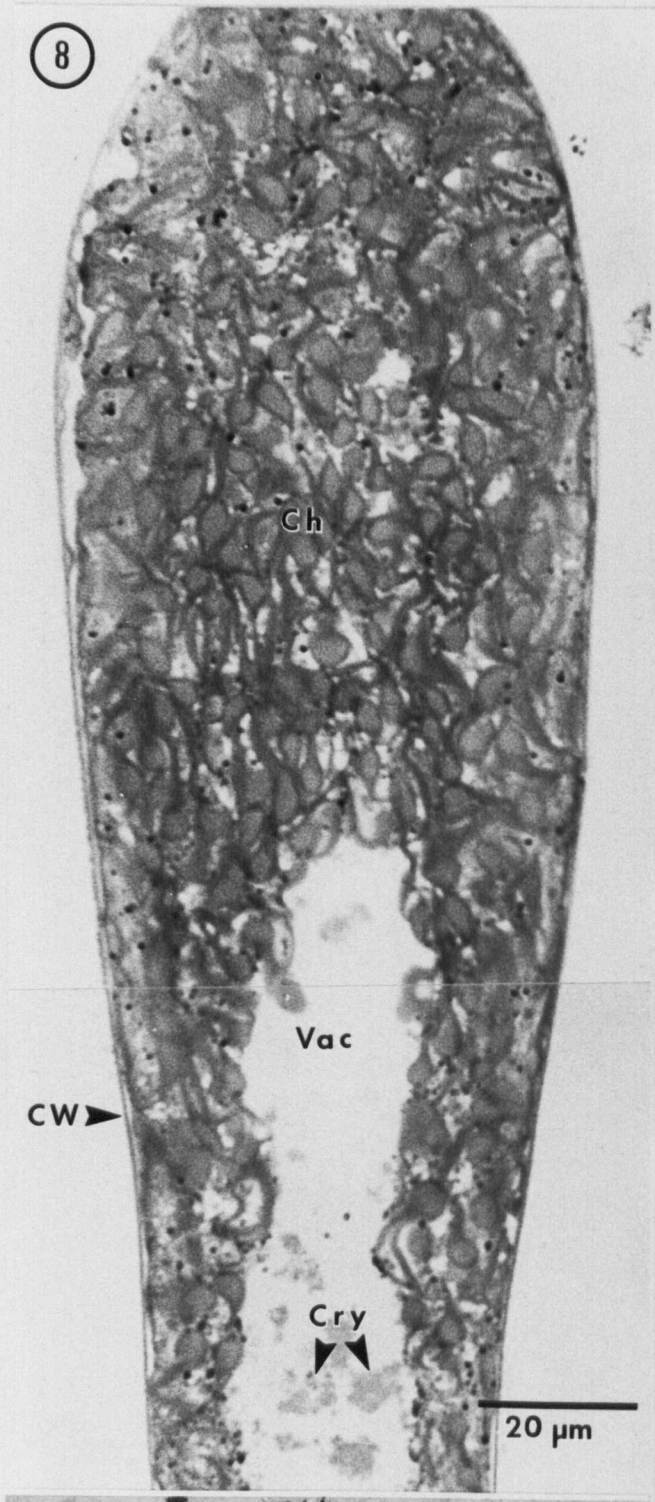
8
Ch
Vac
CW
Cry
20 µm

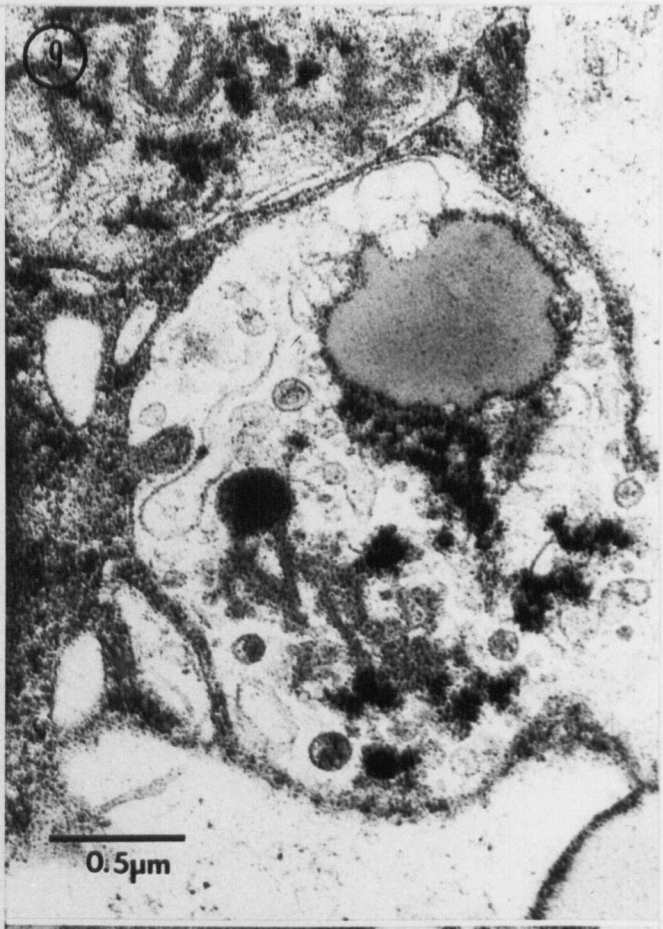
9
0.5µm

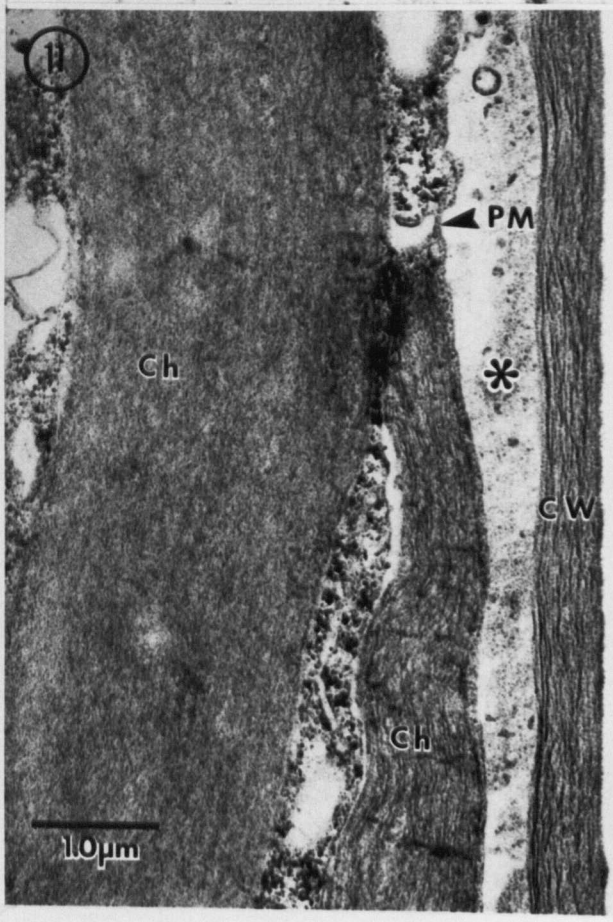
11
PM
Ch
*
CW
Ch
1.0µm

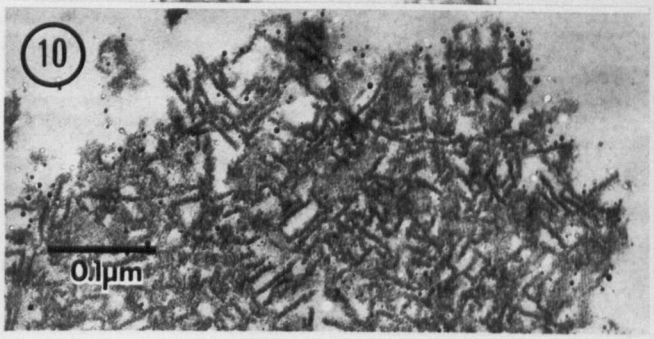
10
0.1µm

Fig. 12. Longitudinal section of the tip of a filament undergoing aplanosporogenesis. Note the infurrowing of the inner wall (arrowheads) and the highly reticulated morphology of the cytoplasm of the developing aplanospore.

Fig. 13. Septation of the aplanospore from the vegetative filament by infurrowing of the inner wall (small arrowheads). The walls of the aplanospore (small arrowheads) and the aplanosporangium (large arrowheads) become clearly distinguishable at this stage.

Fig. 14. Septation is nearly complete with only a small channel of cytoplasmic continuity remaining (arrowhead). Note the re-formation of the central vacuole and the regular arrangement of chloroplasts in the peripheral cytoplasm.

Fig. 15. Final stage in the individualization of the aplanospore from the vegetative filament.

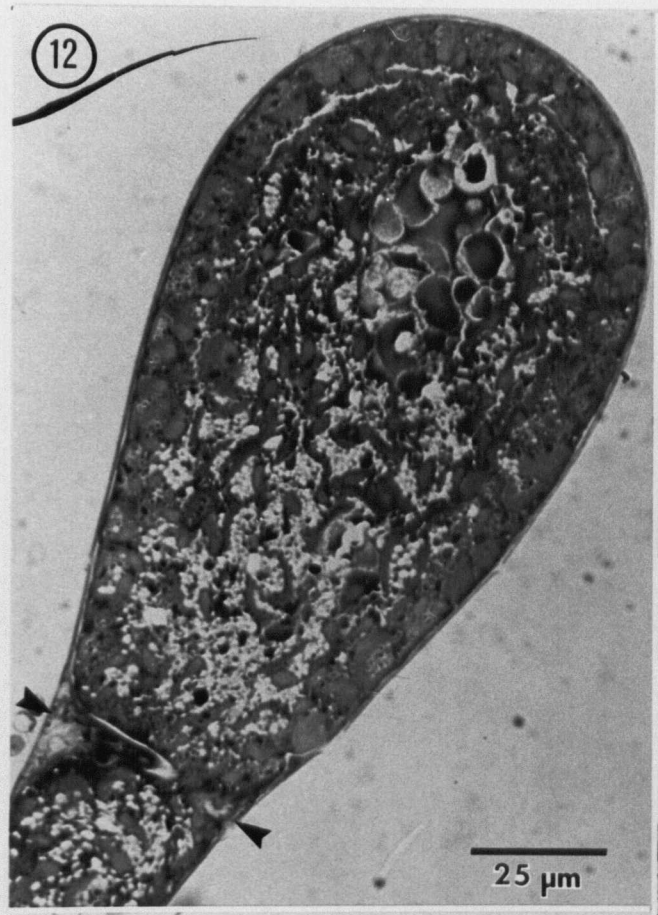
12
25 µm

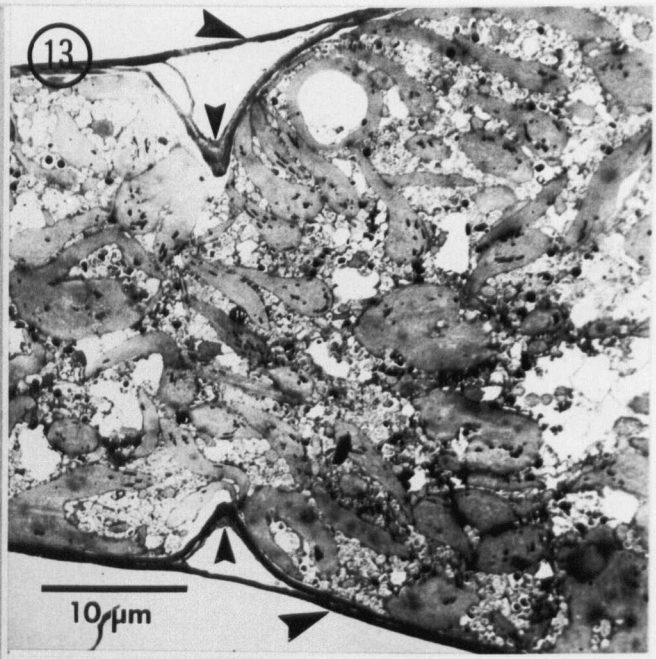
13
10 µm

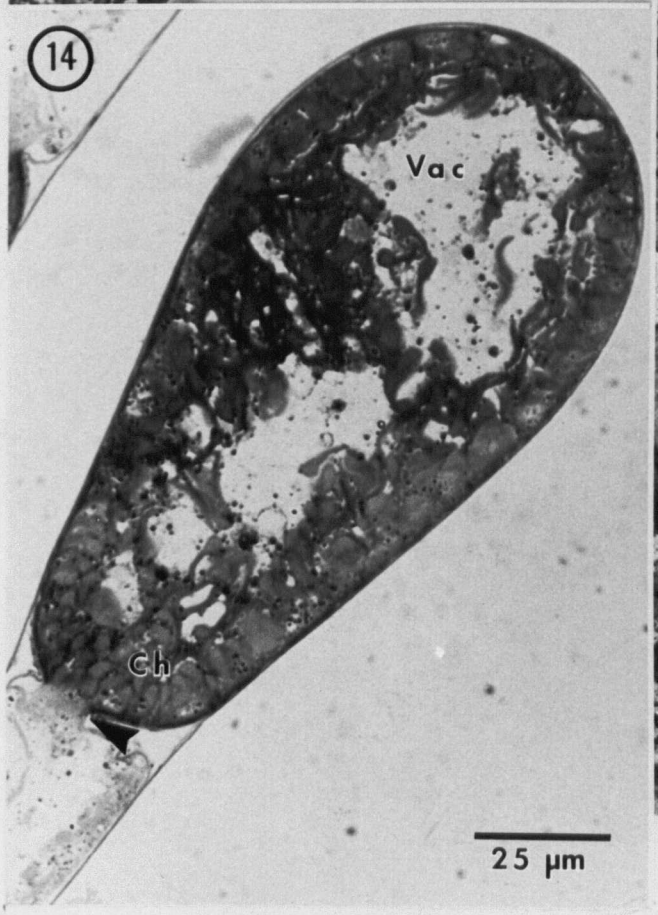
14
Vac
Ch
25 µm


15
ASW
AW
N
N
Ch
Ch
5 µm

Fig. 16. The final stage of aplanosporogenesis showing the individualized walls of the aplanospore (AW) and aplanosporangium (ASW). Mitochondrion-endoplasmic reticulum-dictyosome associations are observed throughout the cytoplasm (arrowheads).

Fig. 17. Detail of the walls of the aplanospore (AW) and the aplanosporangium (ASW). Note the fibrillar material (*) between the walls.

Fig. 18. Chloroplast showing the large pyrenoid penetrated by thylakoids.

Fig. 19. Mature aplanospore within an aplanosporangium. Large numbers of chloroplasts are peripherally arranged and a new central vacuole is coalescing from the smaller vacuoles. The aplanospore wall (AW) and aplsnoaporangium wall (ASW) are easily distinguishable as well.

Fig. 20. Scanning electron micrograph of a mature aplanospore within an aplanosporangium. Isolation of the aplanospore from the vegetative filament is clearly shown.

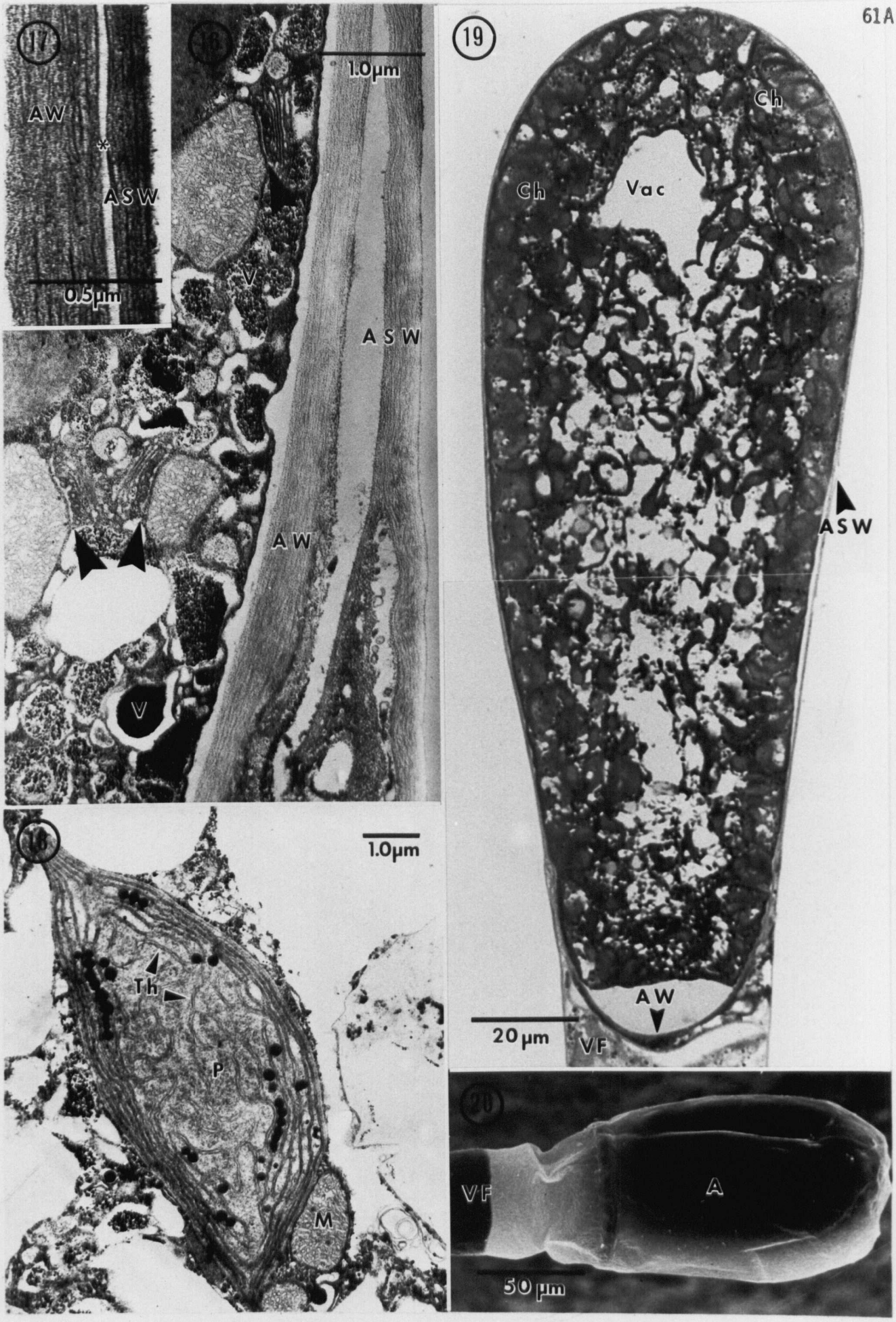
17
AW
*
ASW
0.5µm
18
1.0µm
V
ASW
AW
V
19
Ch
Ch
Vac
ASW
AW
20 µm
VF
18
1.0µm
Th
P
M
20
VF
A
50 µm

Fig. 21 Schematic representation of the most important events in aplanosporogenesis in *V. longicaulis* var. *macounii*.

(A) Vegetative filament prior to aplanosporogenesis. AZ = apical zone; SZ = subapical zone; ZoV = zone of vacuolation.

(B) Early aplanosporogenesis. Note the swelling of the tip, the accumulation of organelles within the tip and the displacement of the central vacoule from the tip.

(C) Infurrowing of the inner wall at the neck of the swollen vegetative filament tip. The new central vacuole begins to coalesce and reform amidst the reticulated cytoplasm and peripherally situated chloroplasts.

(D) Mature aplanosporangium containing a single multinucleated aplanospore. Septation from the vegetative filament is complete; the central vacuole continues to expand.

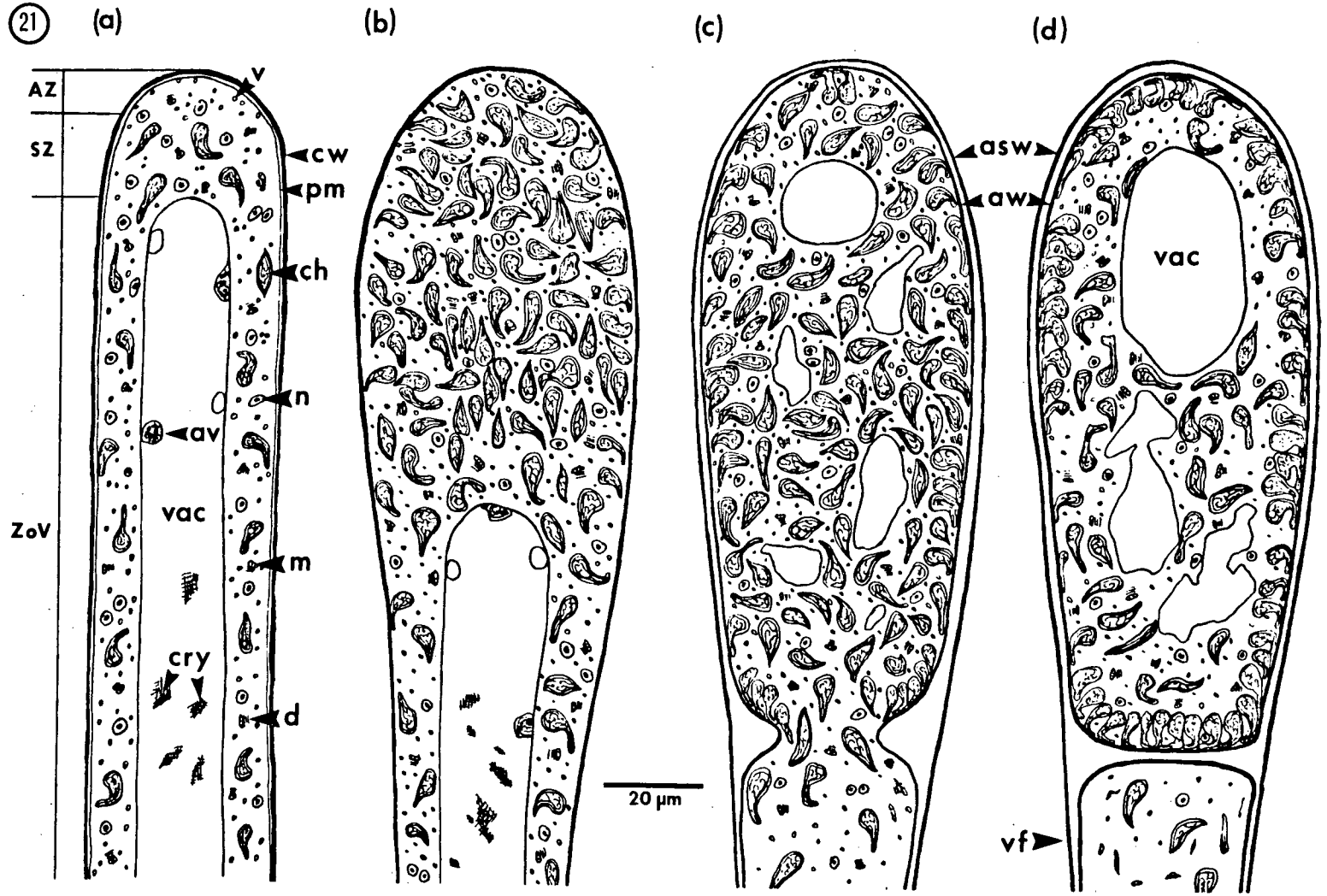
21
(a)
(b)
(c)
(d)
AZ
SZ
ZoV
v
cw
pm
ch
n
av
vac
m
cry
d
20 µm
asw
aw
vac
vf

Fig. 22. Four vegetative filaments are seen emerging from a single aplanospore.

Fig. 23. Aplanospore body emptied of its contents a few days following germination.

Fig. 24. Mature aplanospore just after emergence from an aplanosporangium. A node (large arrowhead) indicates previous aplanospore production. This filament has grown through an aplanosporangium case (small arrowhead).

Fig. 25. Section through a mature aplanospore shortly after release. Chloroplasts are peripherally arranged.

Fig. 26. *In situ* germination of an aplanospore. Two germinating filaments are seen (small arrowheads) along with the aplanosporangium wall casing (large arrowhead).

Fig. 27. Germination of the aplanospore is indicated by a protrusion of the cell wall (arrowheads).

Fig. 28. Section through a germinating aplanospore which has produced two filaments.

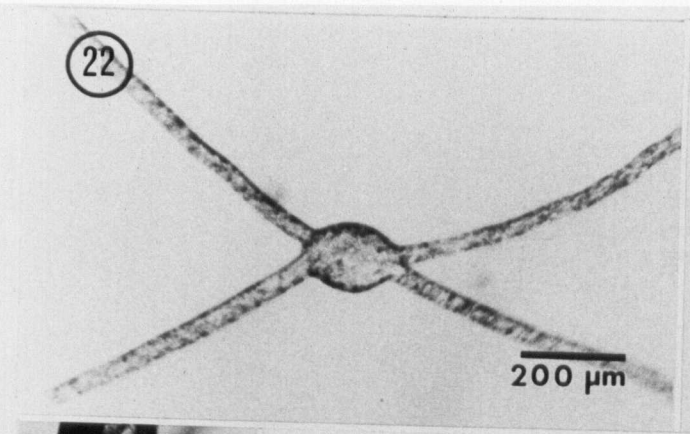
22
200 µm

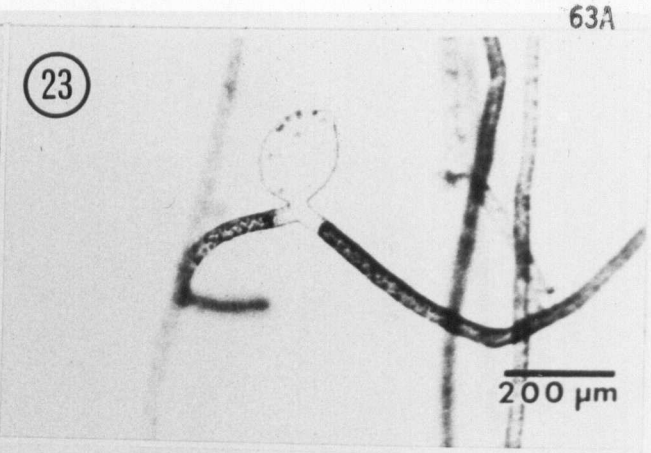
23
200 µm

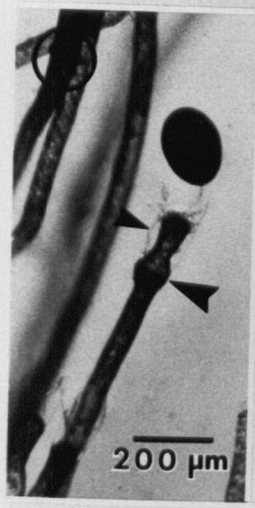
200 µm

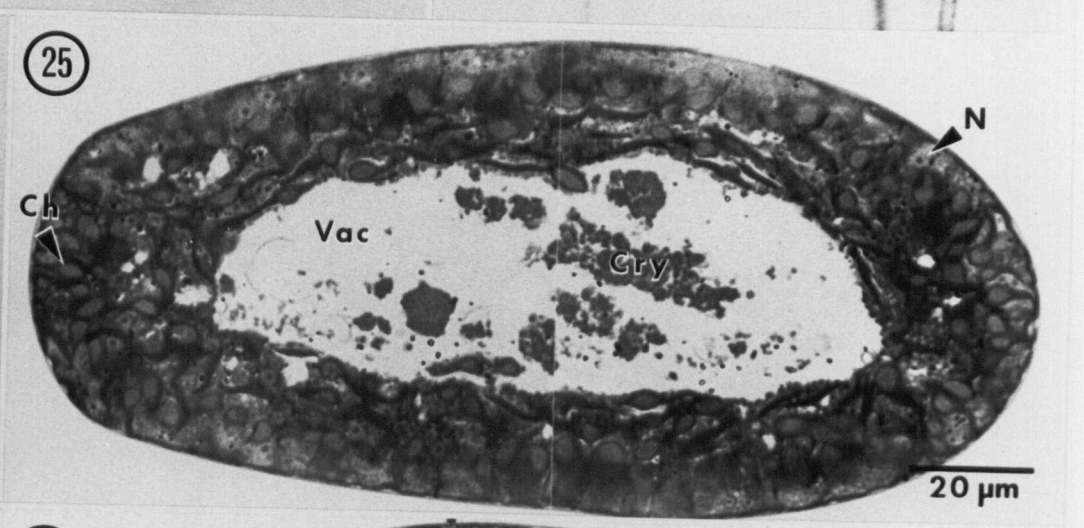
25
N
Ch
Vac
Cry
20 µm

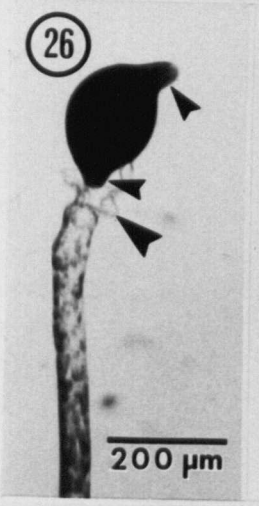
26
200 µm

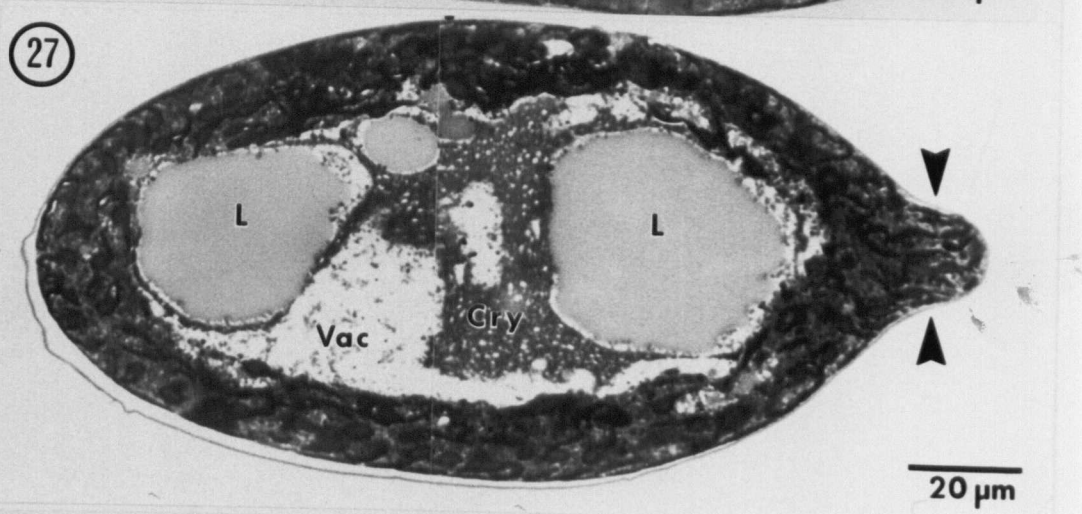
27
L
L
Vac
Cry
20 µm

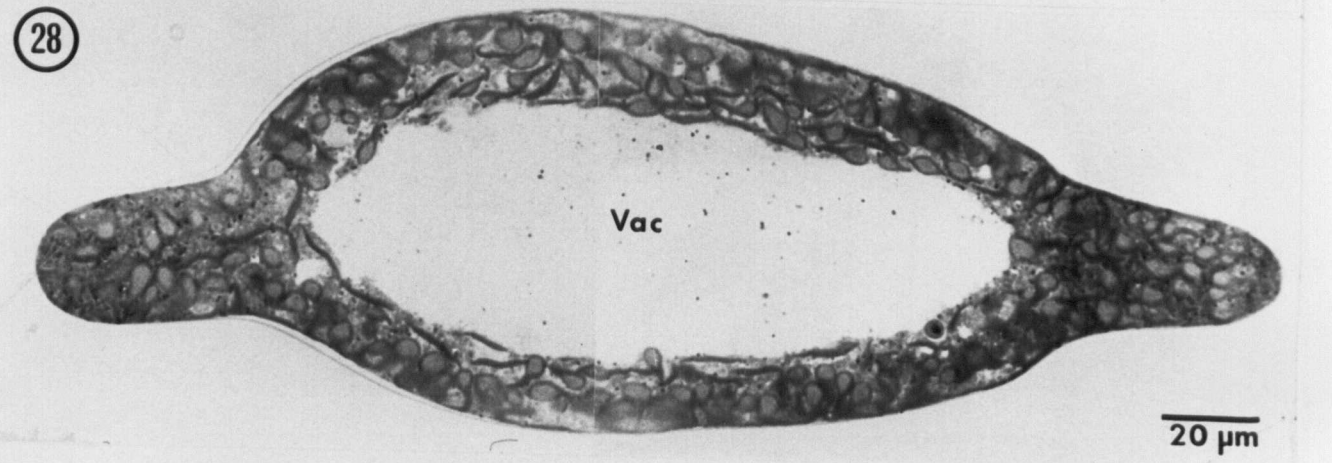
28
Vac
20 µm

Fig. 29. Cell wall of uniform thickness and peripherally arranged chloroplasts characterize the newly released aplanospore (stage I). Note that no signs of release of new wall material is observed.

Fig. 30. Detail of a mitochondrion-ER-dictyosome complex. Two fibrillar-material containing vesicles appear at the trans-cisterna of dictyosomes (arrowheads).

Fig. 31. The protrusion which marks the beginning of germination (stage II) contains many fibrillar-material containing vesicles, nuclei, mitochondria -ER-dictyosome complexes (*) and chloroplasts.

Fig. 32. Detail of the paramural space at the tip of the protrusion. Released materials accumulate in this region and seem to be in the process of being incorporated into the wall.

Fig. 33. Exocytosis of the contents of a single fibrillar-material containing vesicle into the paramural space.

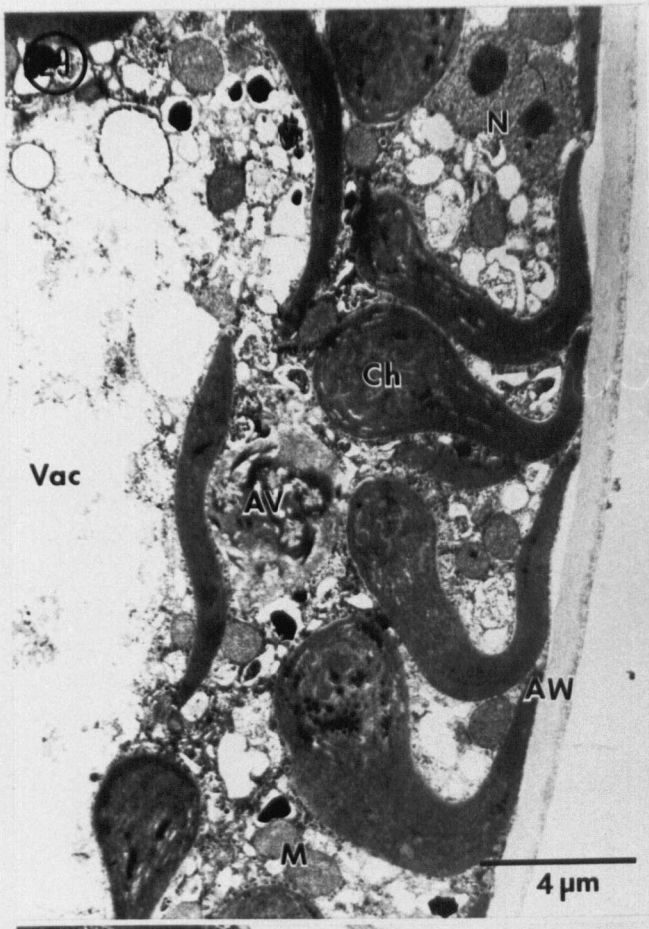
29
N
Ch
Vac
AV
AW
M
4 µm

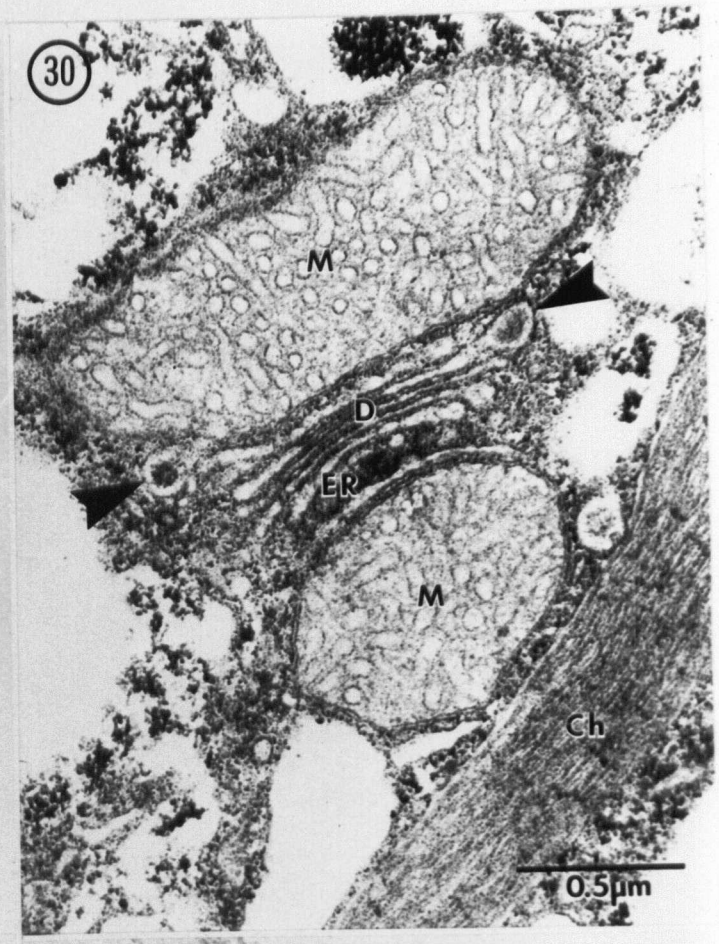
30
M
D
ER
M
Ch
0.5µm

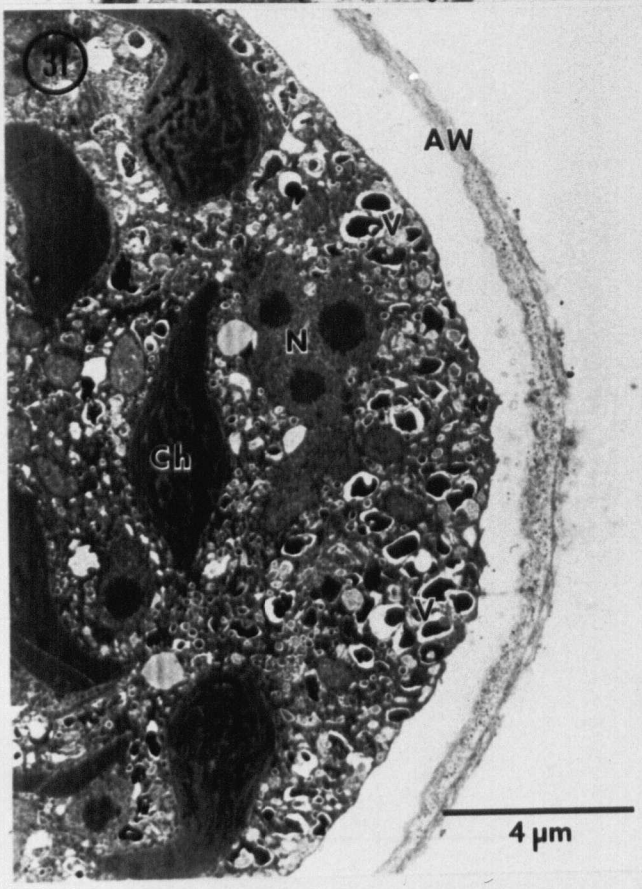
31
AW
V
N
Ch
V
4 µm

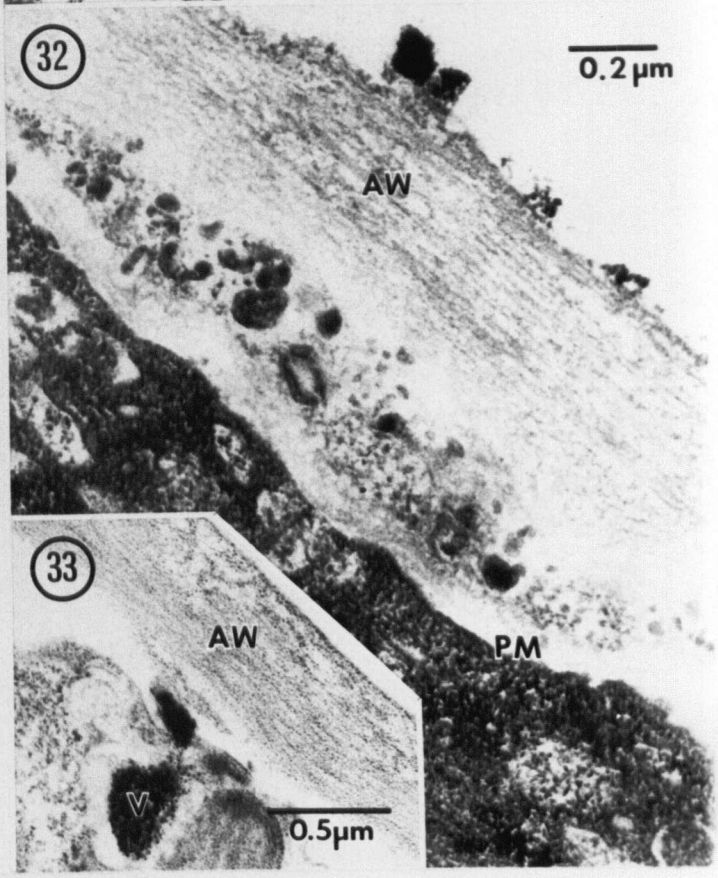
32
0.2 µm
AW
PM
33
AW
V
0.5µm

Fig. 34. Small bundle of microtubules in the cytoplasm of an an aplanospore prior to germination (arrowheads). Note that these microtubule bundles are not positioned parallel to the plasma membrane.

Fig. 35. Bundle containing numerous microtubules showing preferential orientation parallel to the plasma membrane of a germinating aplanospore (arrowheads). Note the proximity of this bundle to one of the nuclei.

Fig. 36. Clusters of endophytic bacteria adjacent to a nucleus. No obvious morphological damage due to the presence of the bacteria is observed.

Fig. 37. A vacuole with four partially digested bacteria.

Fig. 38. Single bacterium embedded in the cell wall of an aplanospore. Note the clear region surrounding the bacterium (*), indicative of the digestion of the aplanospore wall materials.

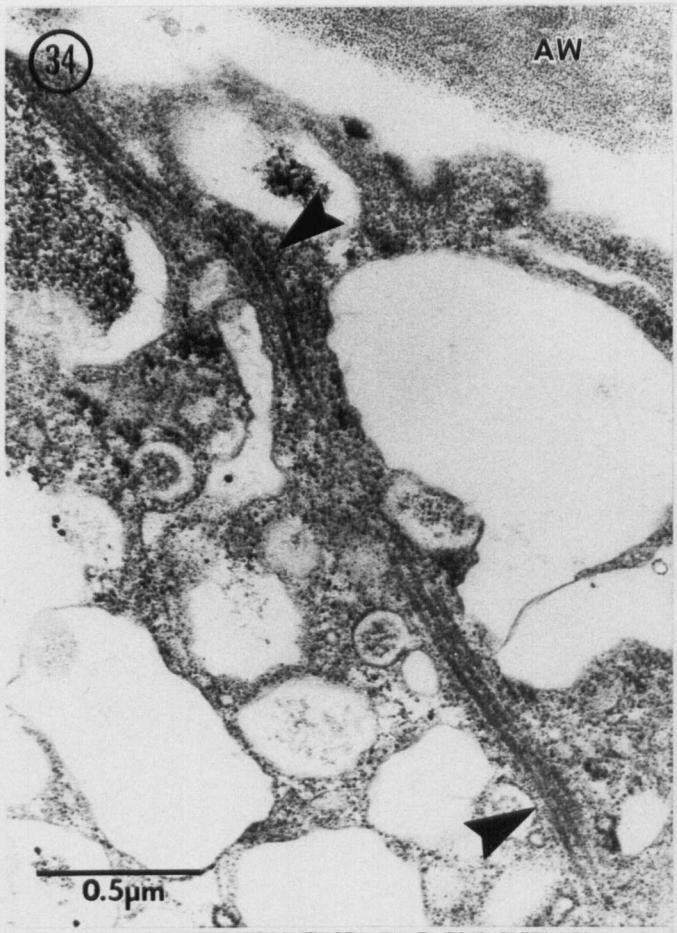
34
AW
0.5μm

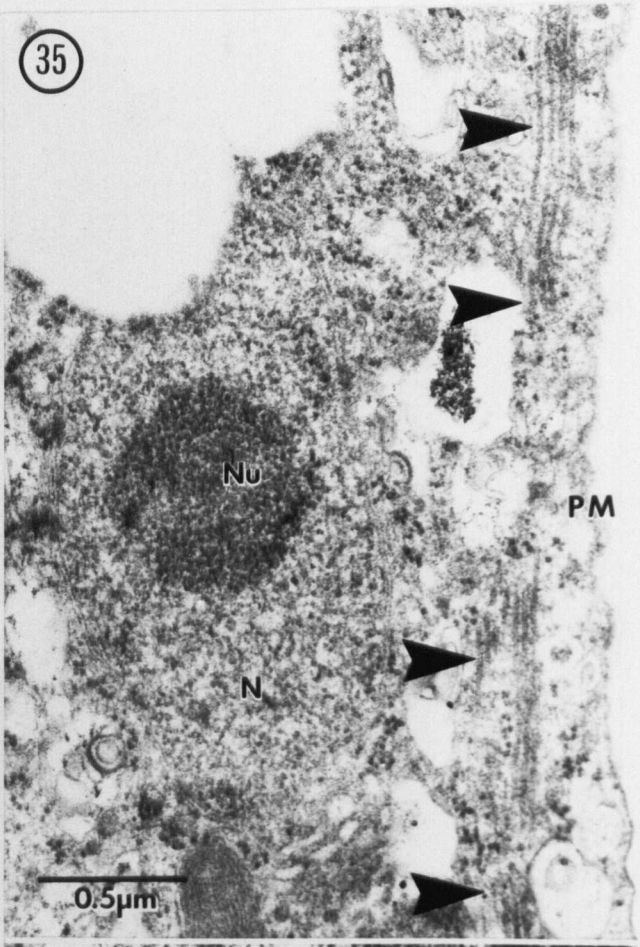
35
Nu
PM
N
0.5μm

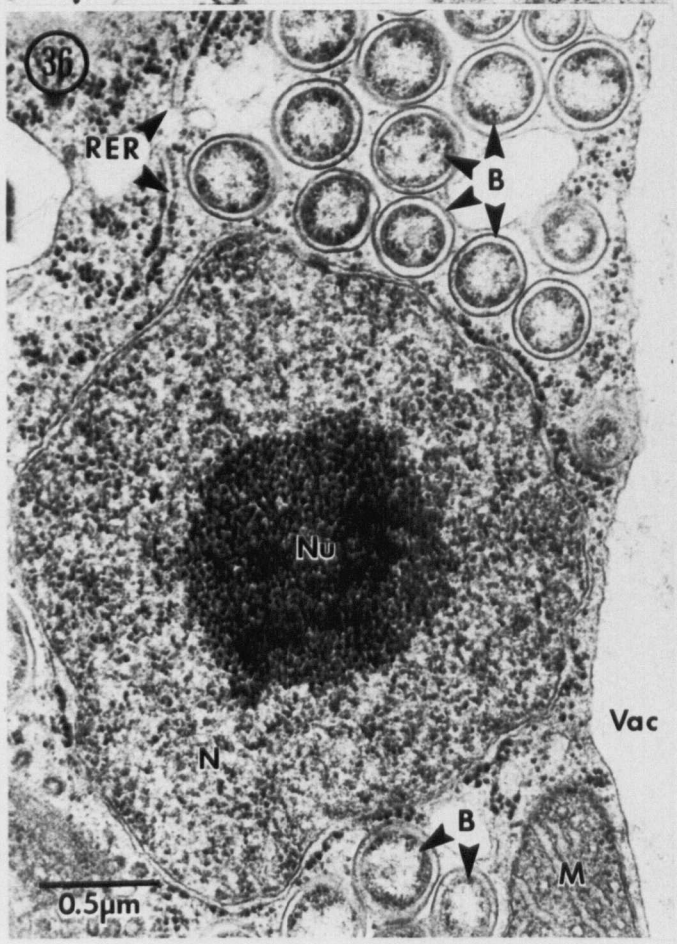
36
RER
B
Nu
Vac
N
B
M
0.5μm

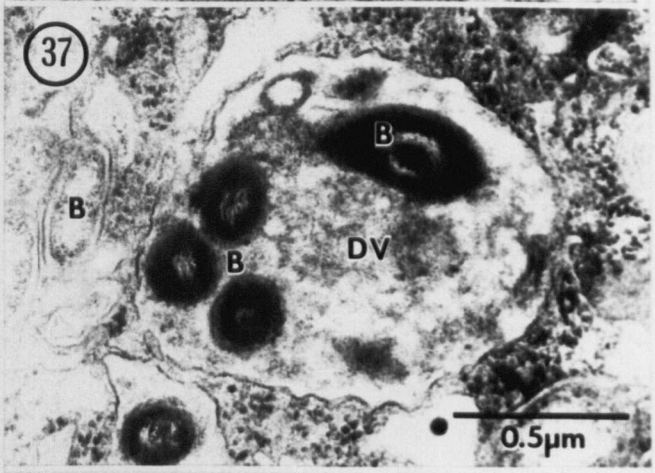
37
B
B
B
DV
0.5μm

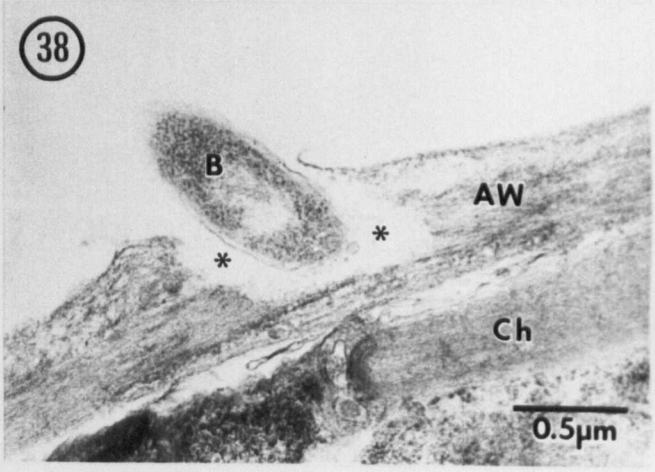
38
B
AW
*
*
Ch
0.5μm

Fig. 39 Volume density of major aplanospore compartments during germination (data from light microscopy sections).

FIGURE 39

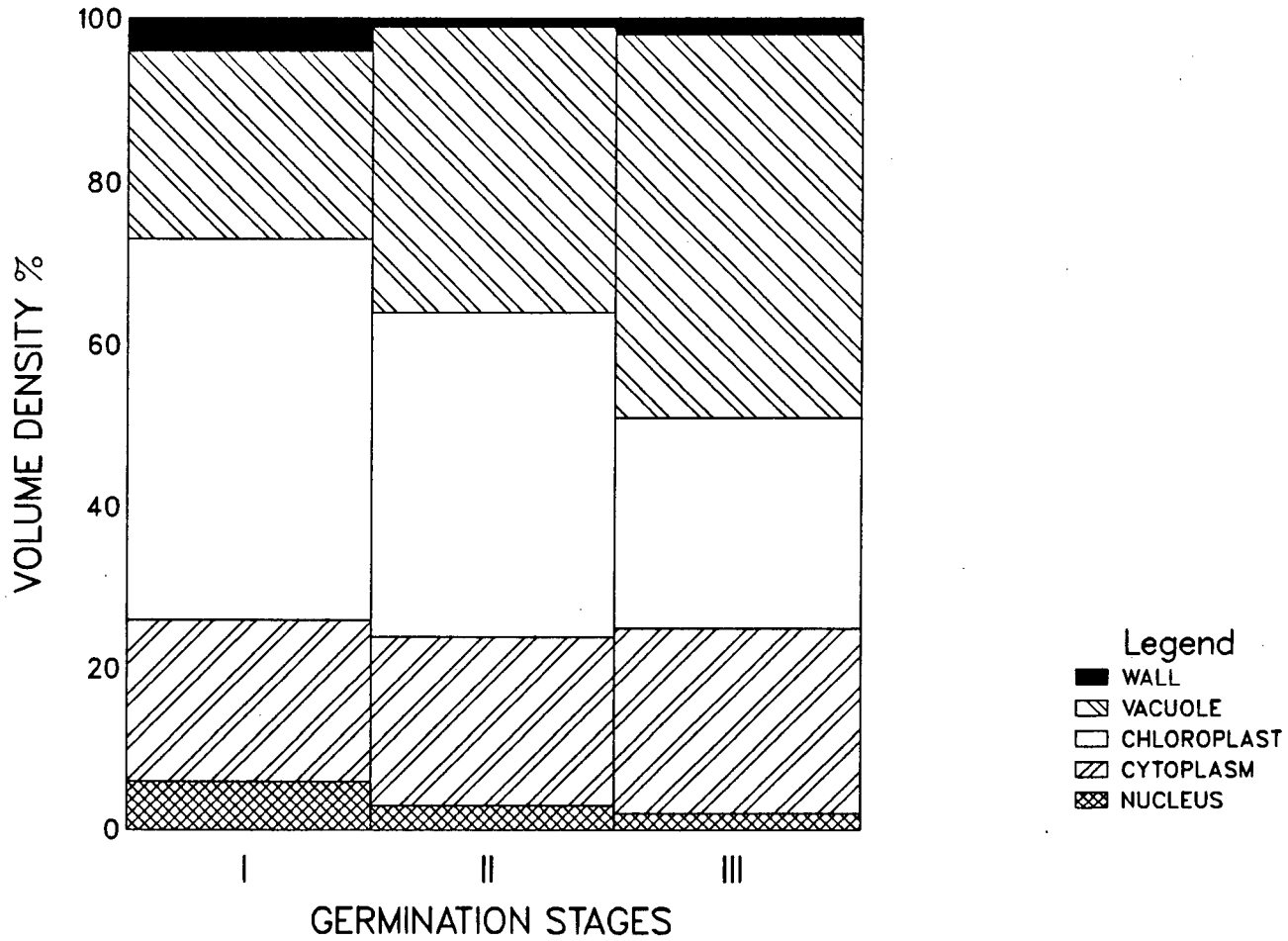
100
80
60
40
20
0
VOLUME DENSITY %
I
II
III
GERMINATION STAGES
Legend
WALL
VACUOLE
CHLOROPLAST
CYTOPLASM
NUCLEUS

Fig. 40 Volume density changes occurring during aplanospore germination in cytoplasmic compartments (data from electron microscopy sections).

FIGURE 40

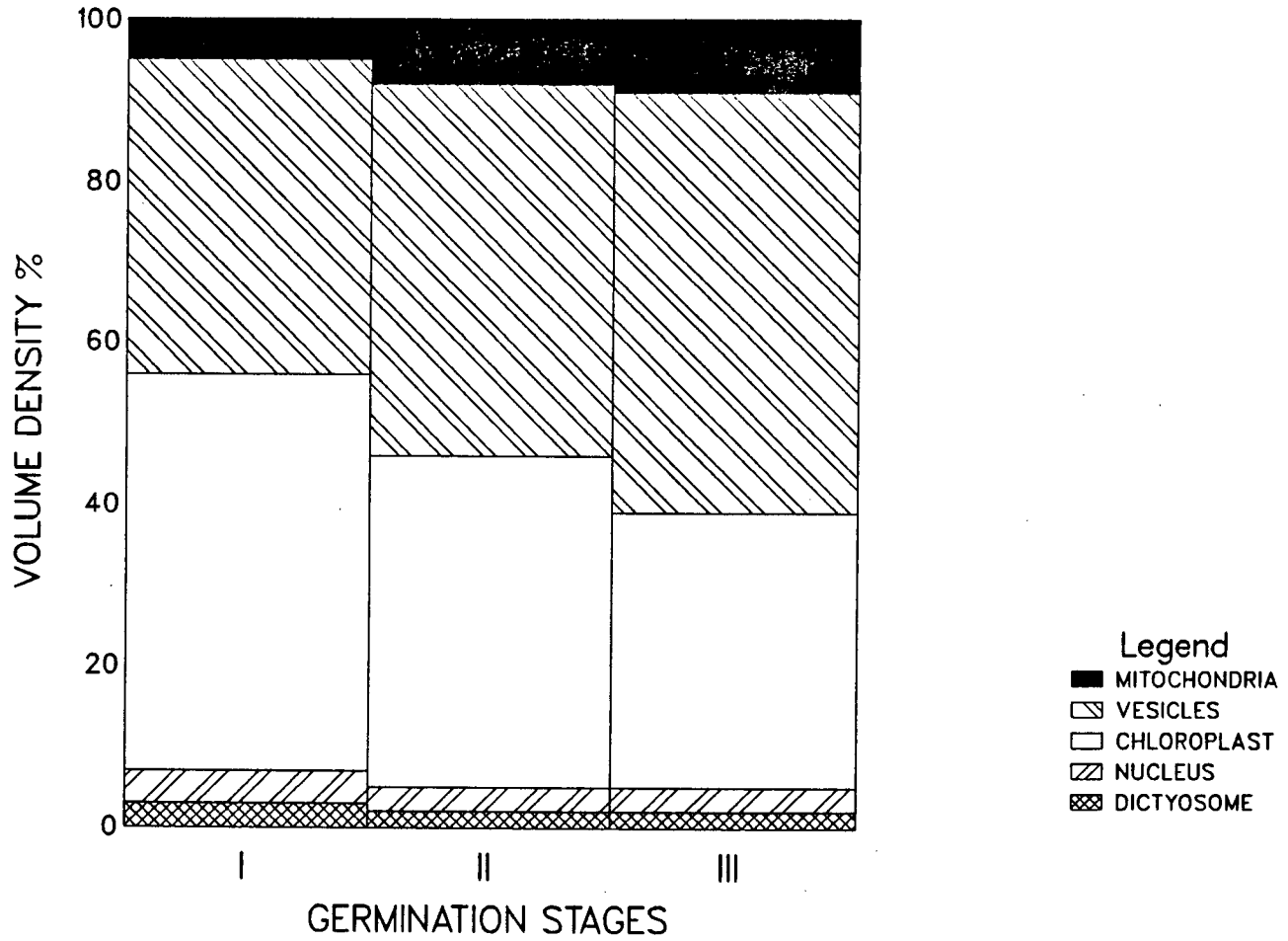
100
80
60
40
20
0
VOLUME DENSITY %
I
II
III
GERMINATION STAGES
Legend
MITOCHONDRIA
VESICLES
CHLOROPLAST
NUCLEUS
DICTYOSOME

Figure 41. Graph showing the effect of CTC concentration on the total filament length at 6 hours and 24 hours after germination.

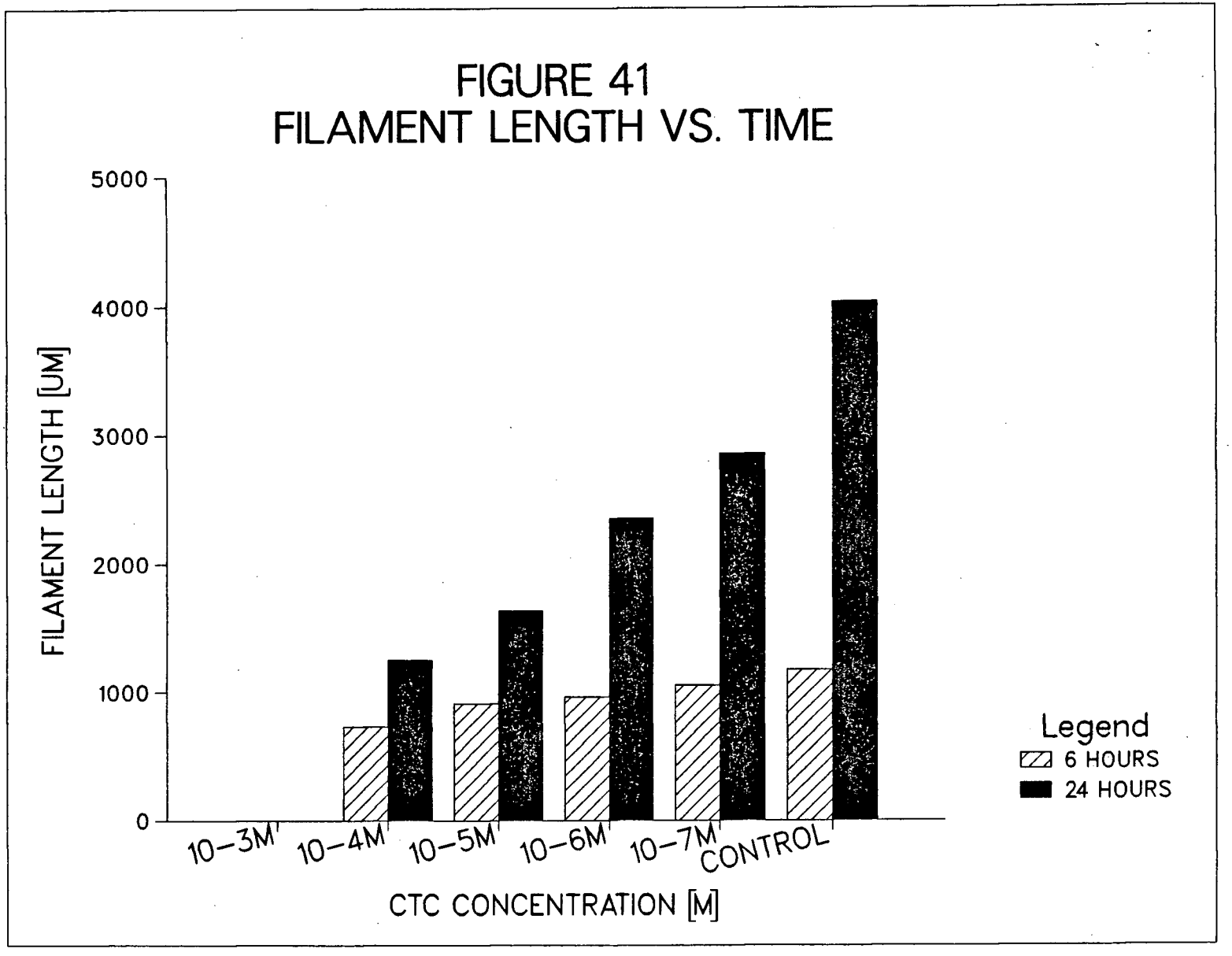
FIGURE 41
FILAMENT LENGTH VS. TIME
FILAMENT LENGTH [UM]
5000
4000
3000
2000
1000
0
10-3M
10-4M
10-5M
10-6M
10-7M
CONTROL
CTC CONCENTRATION [M]
Legend
6 HOURS
24 HOURS

Figure 42. Graph showing the effect of CTC concentration on the growth rate of filaments at 2, 4 and 6 hours of germination.

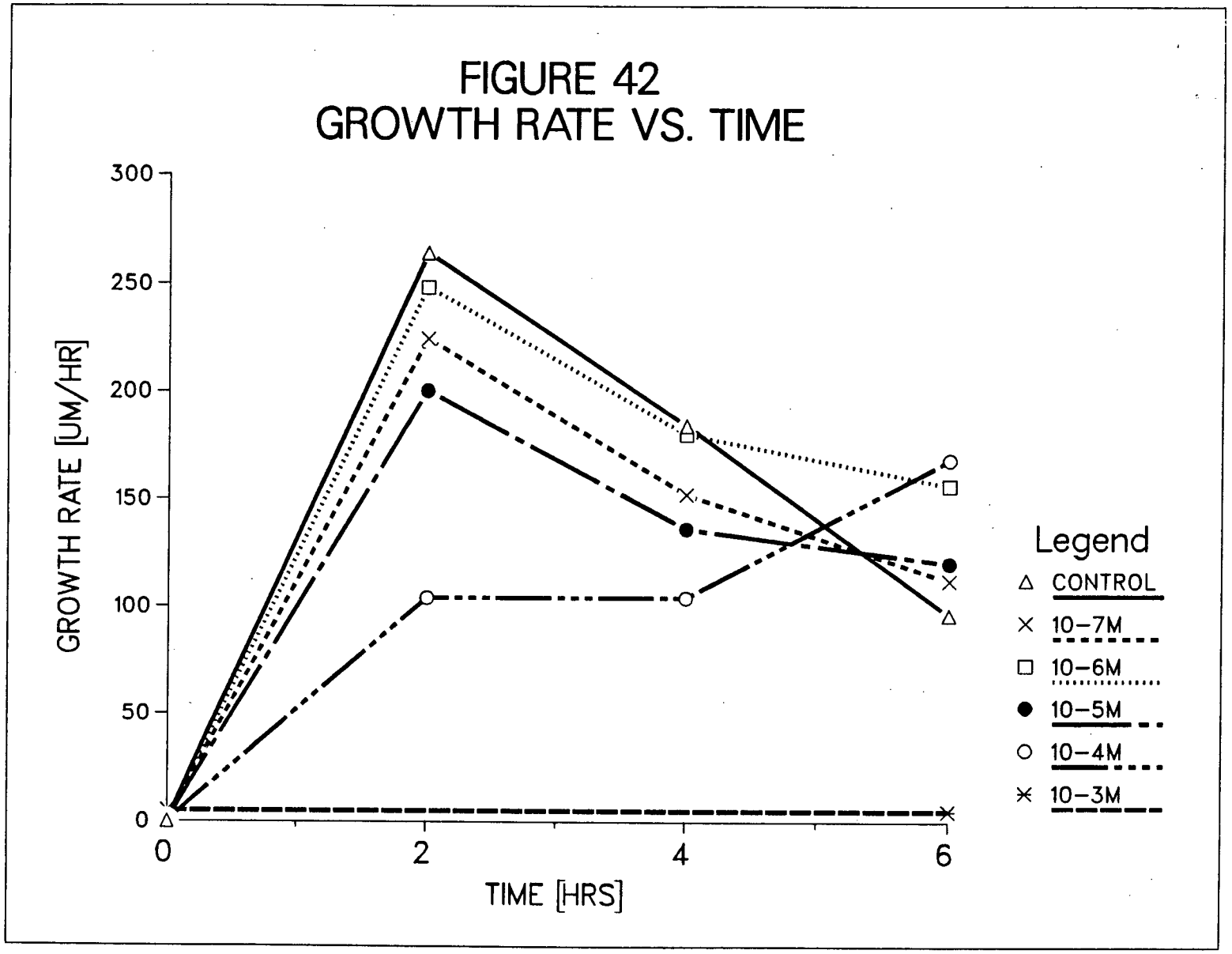
FIGURE 42
GROWTH RATE VS. TIME
GROWTH RATE [UM/HR]
300
250
200
150
100
50
0
0
2
4
6
TIME [HRS]
Legend
CONTROL
10-7M
10-6M
10-5M
10-4M
10-3M

Figure 43. Graph showing the area of the germinating filament reoccupied by CTC fluorescence.

FIGURE 43

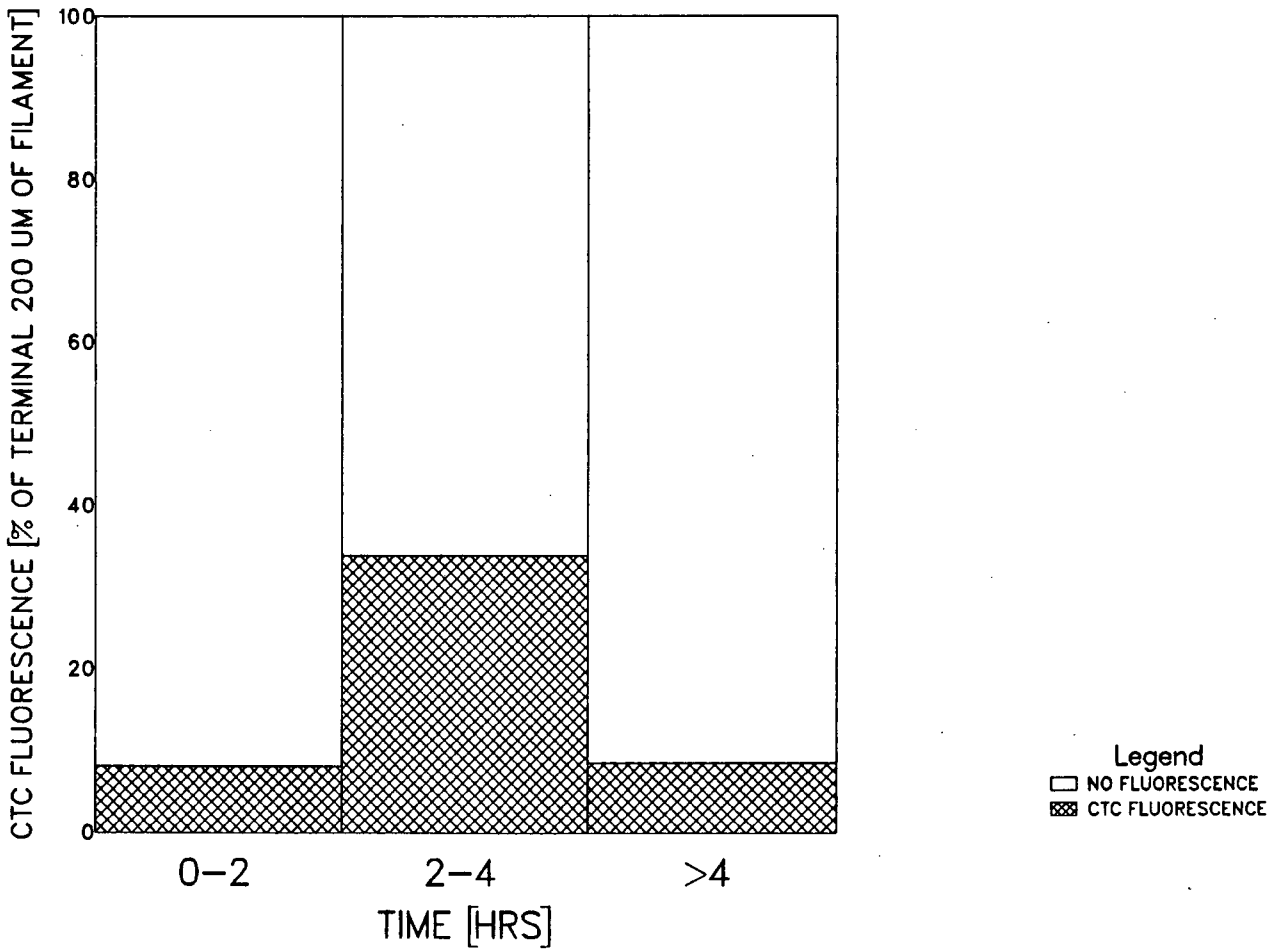
CTC FLUORESCENCE [% OF TERMINAL 200 UM OF FILAMENT]
100
80
60
40
20
0
0–2
2–4
>4
TIME [HRS]
Legend
NO FLUORESCENCE
CTC FLUORESCENCE

Figure 44. Graph showing the distribution and intensity of CTC fluorescence along the 200 μm terminal portion of the germinating filaments.

FIGURE 44

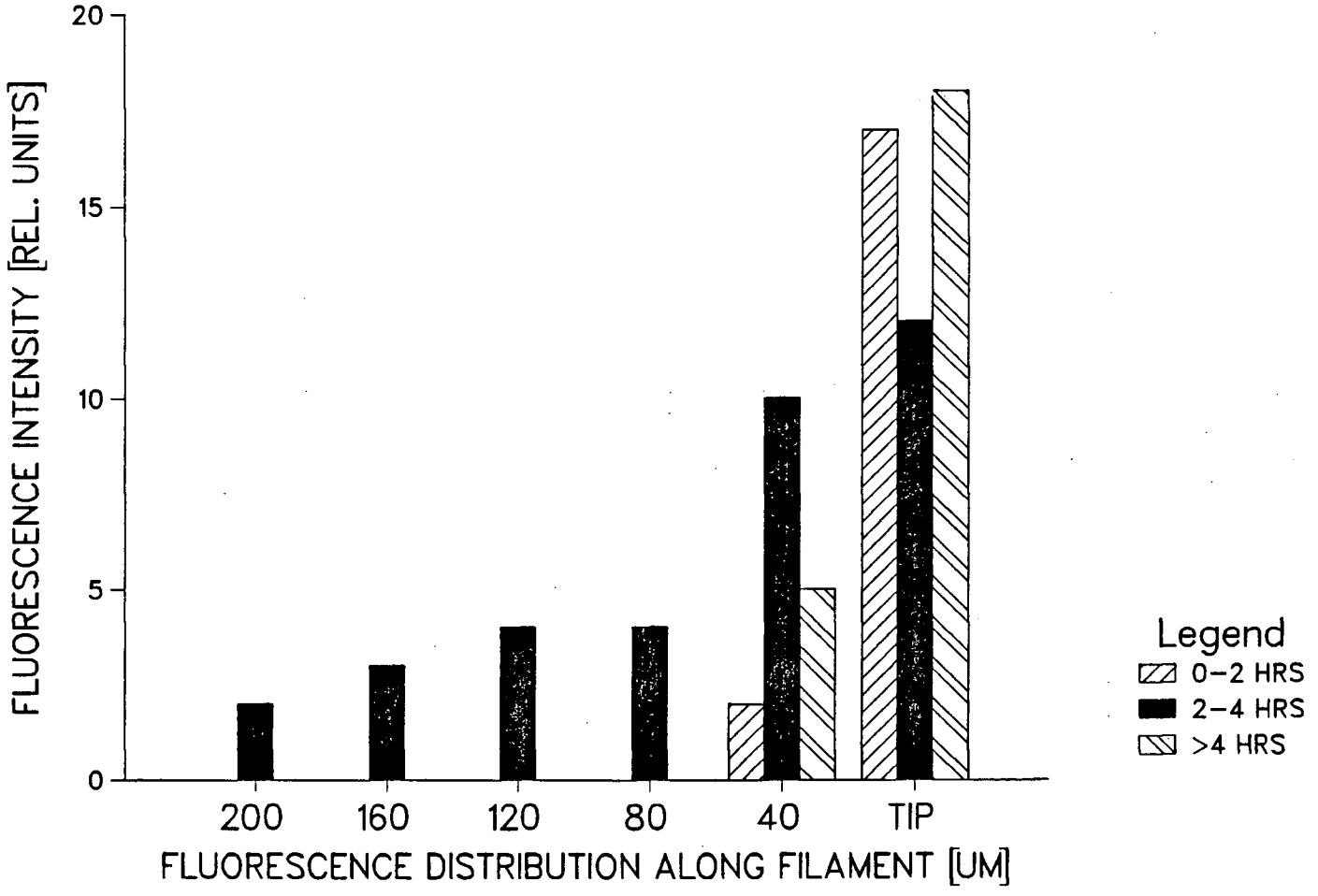
FLUORESCENCE INTENSITY [REL. UNITS]
20
15
10
5
0
200
160
120
80
40
TIP
FLUORESCENCE DISTRIBUTION ALONG FILAMENT [UM]
Legend
0–2 HRS
2–4 HRS
>4 HRS

Figure 45. Light micrograph of filaments grown for 24 hours in CTC-free medium.

Figure 46. Light micrograph of filaments grown for 24 hours in 10^{-4}M CTC. Morphology and branching patterns are similar to those of the control (compare with Fig. 45).

Figure 47. Light micrograph of a germinating aplanospore. Note the regions of low optical density characteristic of the germination sites (arrowheads).

Figure 48. CTC fluorescence of the aplanospore depicted from Fig. 47. The most intense fluorescence is localized at the sites of low optical density.

Figure 49. Light micrograph of an aplanospore exposed to the Ca^{2+}-insensitive probe OTC. No fluorescence is detected with this treatment.


45
400 µm

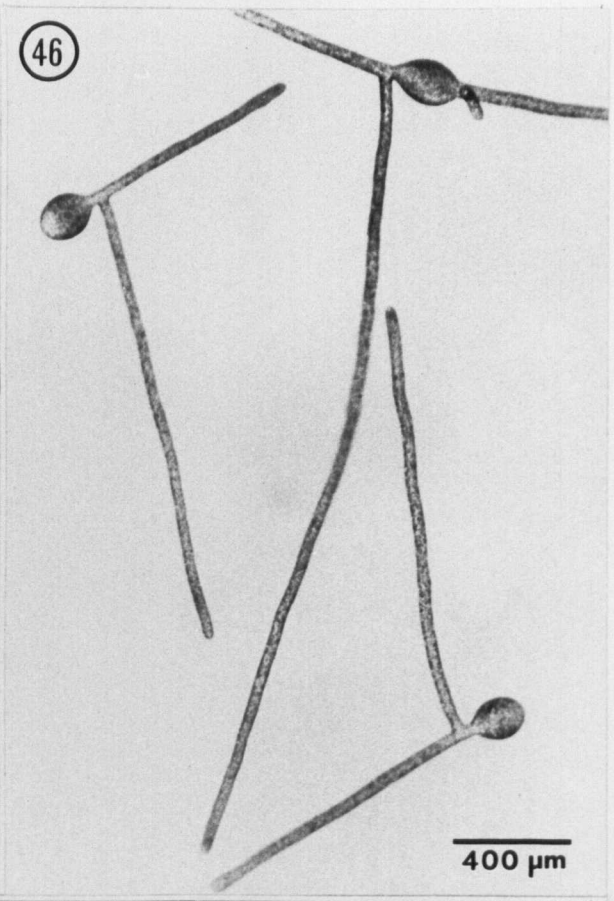
46
400 µm

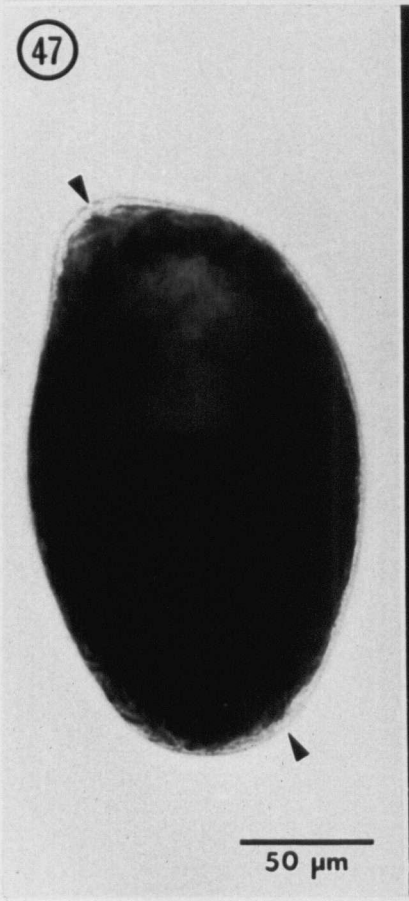
47
50 µm

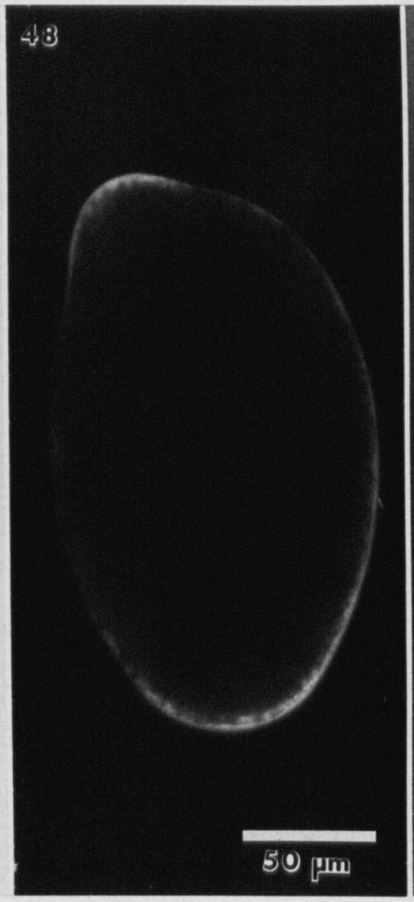
48
50 µm

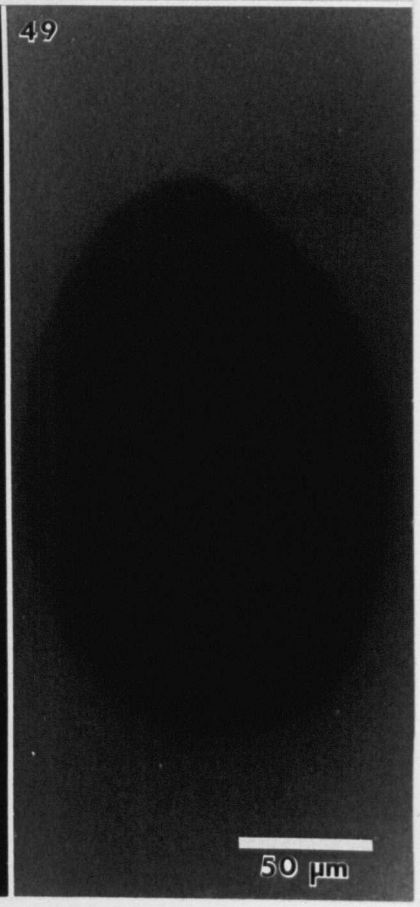
49
50 µm

Figure 50. Tip-localized fluorescence in a filament exposed to 10^{-4}M CTC two hrs after the initiation of germination.

Figure 51. Micrograph of a filament exposed to 10^{-5}M CTC during the transition period from 0-2 to 2-4 hours after the initiation of germination. CTC fluorescence is less localized.

Figure 52. Aplanospore shortly after the initiation of germination. CTC is sharply delimited to the germination site.

Figure 53. Sharply-delimited CTC fluorescence is shown localized at the tip of a filament 4 hours after germination. This pattern is similar to that observed during the first two hours of germination (compare with Figs 50 and 52).

Figure 54. A more diffuse pattern of CTC fluorescence is seen extending basipetally from the tip in filaments between two to four hours after the initiation of germination.

Figure 55. The pattern of CTC fluorescence shown here in a freshly collected vegetative filament.

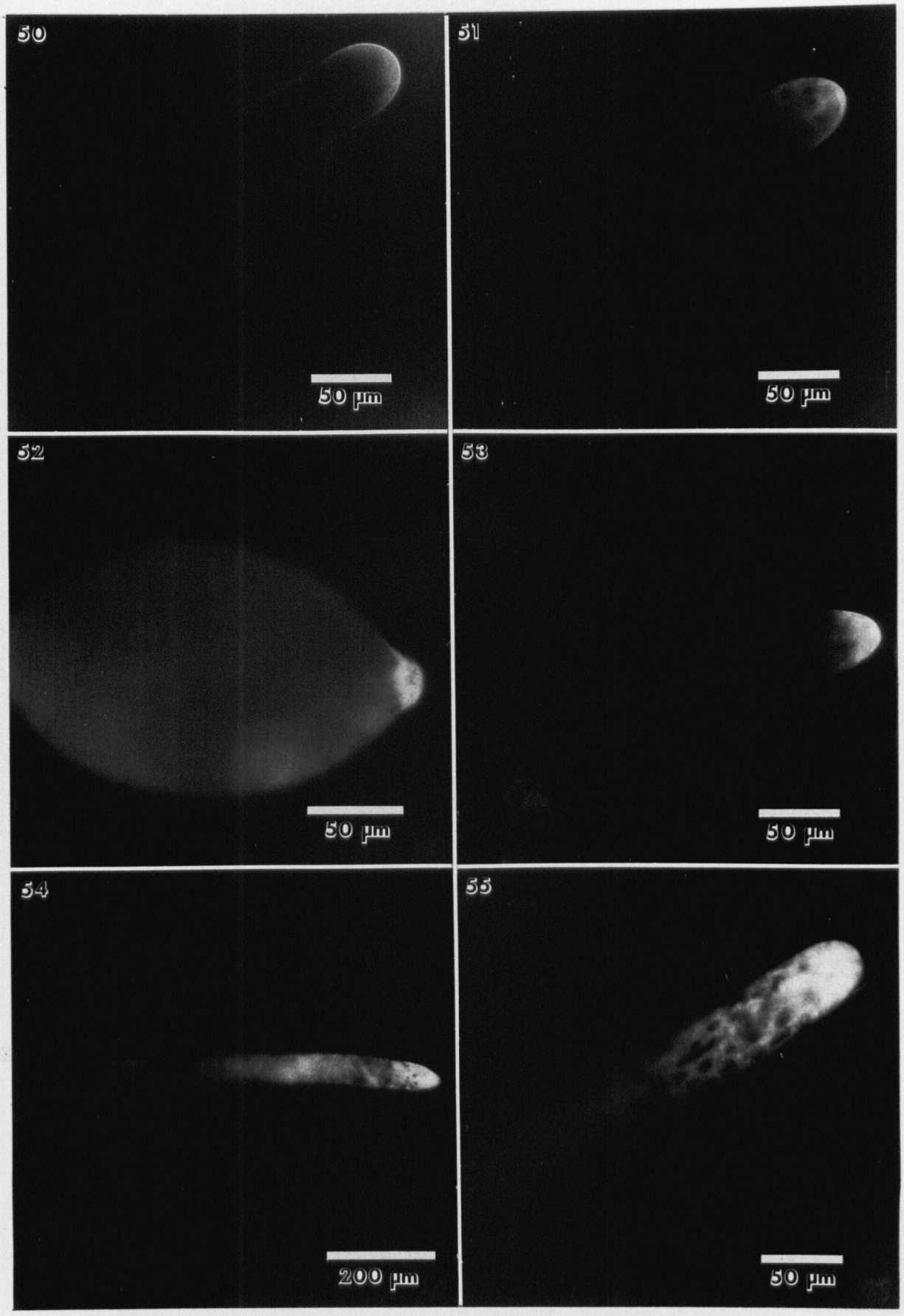
50
50 μm
51
50 μm
52
50 μm
53
50 μm
54
200 μm
55
50 μm

Figure 56. Graph showing the effect of various concentrations of EGTA on the growth rate of newly germinated *Vaucheria* filaments.

Figure 57. Graph showing the effect of various concentrations of calcium ionophore A23187 on the growth rate of newly germinated *Vaucheria* filaments.

Figure 58. Graph showing the effect of various concentrations of the calmodulin antagonist TFP on the growth rate of newly germinated *Vaucheria* filaments.

Figure 59. Graph comparing the results of the effects of all three compounds (EGTA, A23187 and TFP) on the growth rate of newly germinated *Vaucheria* filaments.

FIGURE 56
EGTA GROWTH RATES

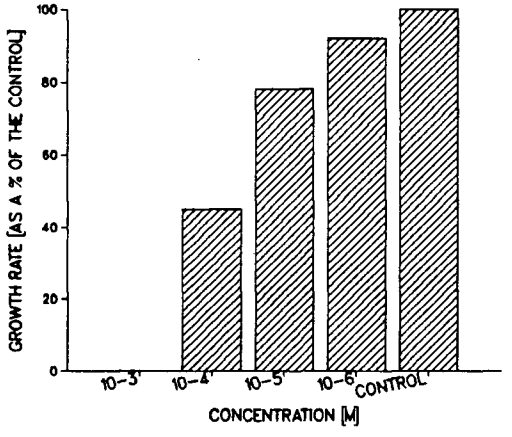

FIGURE 57
A23187 GROWTH RATES

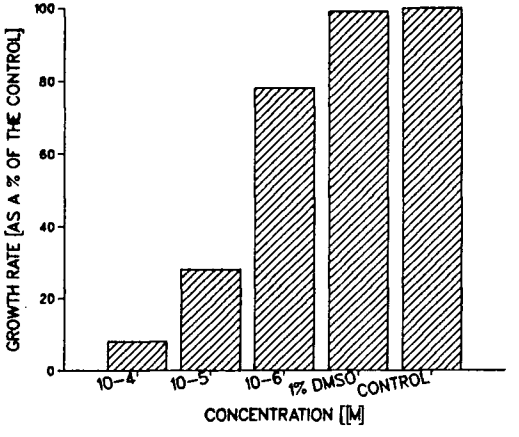

FIGURE 58
TFP GROWTH RATES

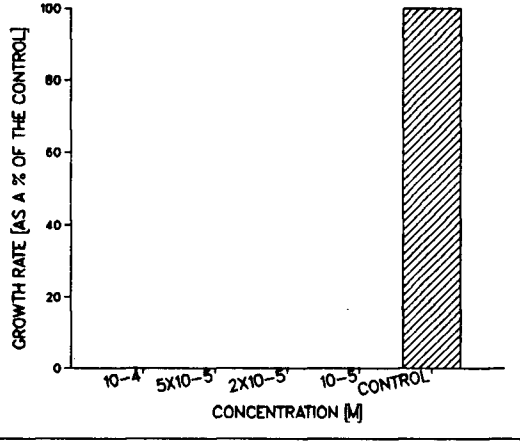

FIGURE 59
GROWTH RATES VS. CONCENTRATION

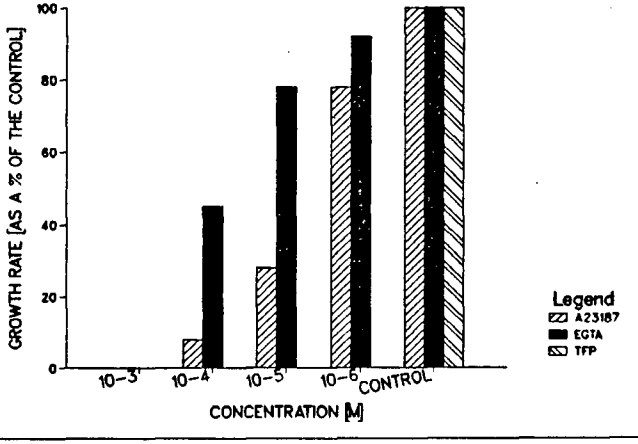

Figure 60. Micrograph of a germinating filament from an aplanospore incubated in untreated medium.

Figure 61. Same specimen as in Fig. 60, 10 minutes after incubation with 10^{-4}M CTC.

Figure 62. Micrograph of a germinating filament from an aplanospore incubated in 10^{-4}M EGTA.

Figure 63. Same specimen as in Fig. 62, 10 minutes after incubation with 10^{-4}M CTC. Fluorescence is less intense and more diffuse than in the untreated material (compare with Fig. 61).

Figure 64. Micrograph of germinating filaments from an aplanospore incubated in 10^{-4}M A23187. Note the disoriented growth pattern, apical swellings, bud-like protrusions and regions low optical density (arrowheads).

Figure 65. Micrograph of germinating filaments from an aplanospore incubated in 10^{-4}M A23187, followed by 10^{-4}M CTC. Note the bright fluorescence at the swollen tip (arrowhead).

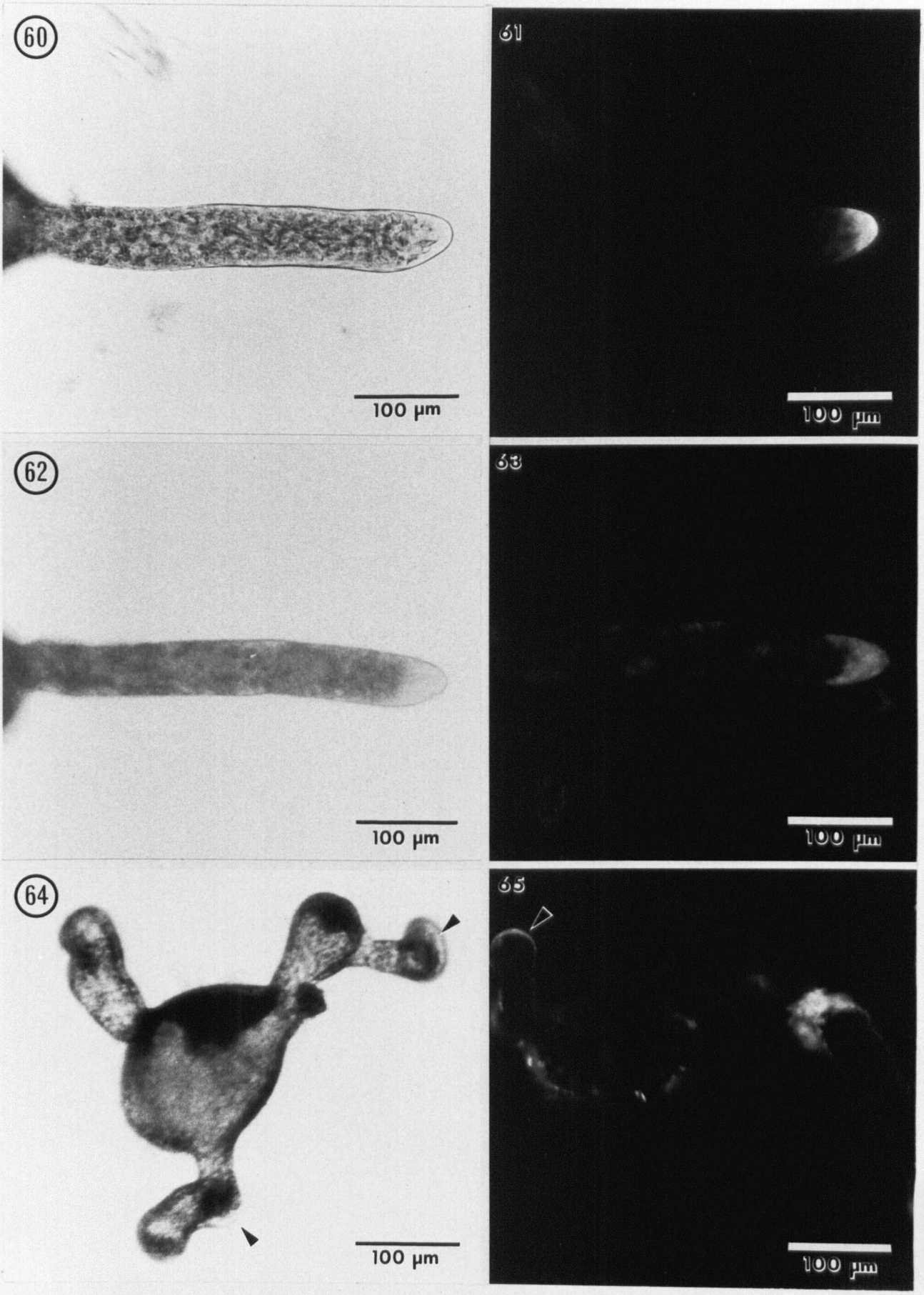
60
100 µm
61
100 µm
62
100 µm
63
100 µm
64
100 µm
65
100 µm

Figure 66. Micrograph of germinating filaments from aplanospores incubated in 10^{-5}M A23187. Irregular filament diameters, swollen apices and protrusions are still present.

Figure 67. Micrograph of germinating filaments from aplanospores incubated in 10^{-6}M A23187. The only abnormality observed is filament diameters of irregular width.

Figure 68. Micrograph of germinating filaments from aplanospores incubated in 1% DMSO. No morphological abnormalities are seen.

Figure 69. Micrograph of a single aplanospore incubated in 10^{-5}M TFP, 10 minutes after 10^{-4}M CTC application. No signs of fluorescence is detected after incubation with CTC.

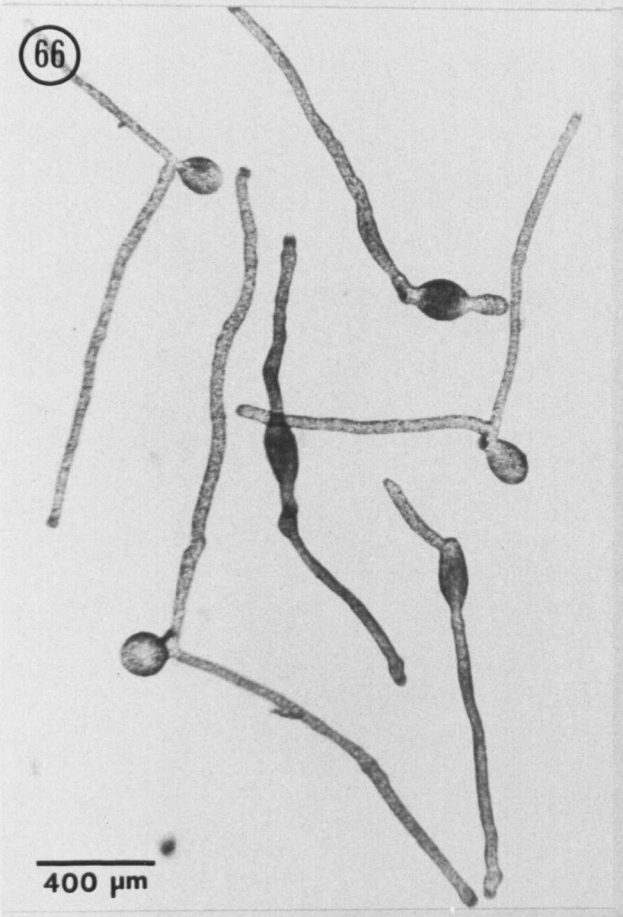
66
400 µm

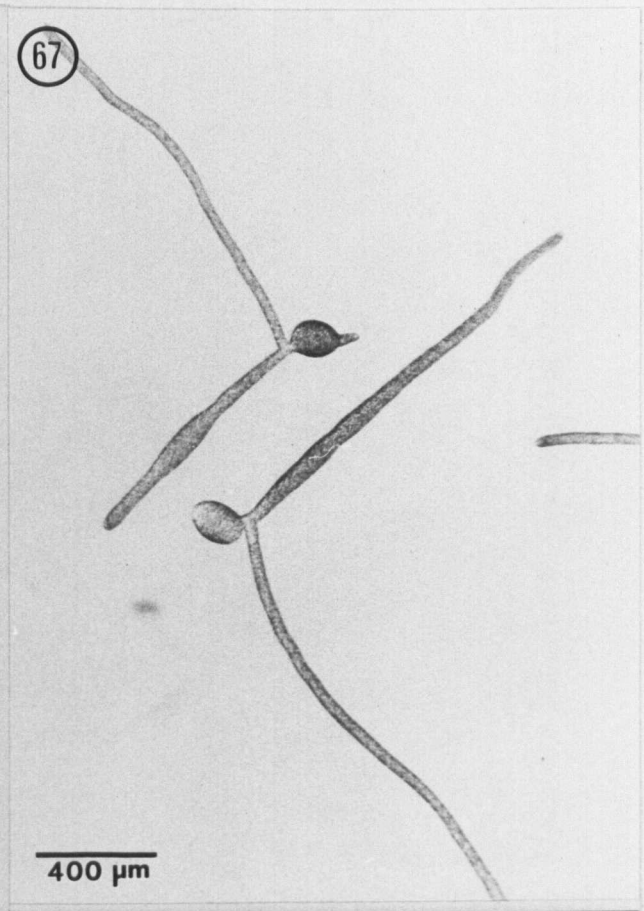
67
400 µm

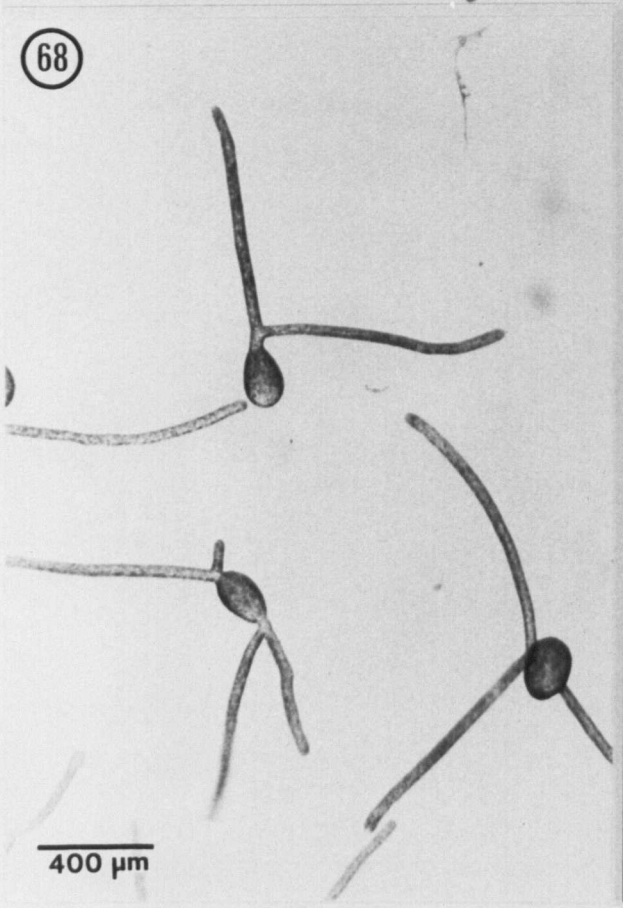
68
400 µm

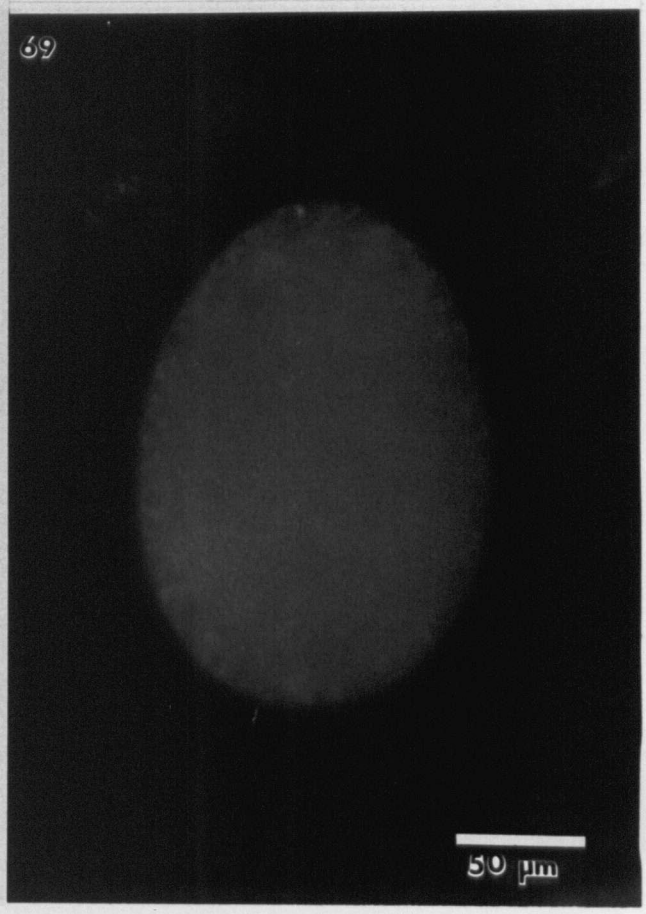
69
50 µm

Aghajanian, J.G. 1979. A starch grain-mitochondrion-dictyosome association in Batrachospermum (Rhodophyta). J. Phycol. 15: 230-232.

Al-Khazzar, A.R., M.J. Earnshaw, R.D. Butler, M.J. Emes and D.C. Sigee. 1984. Tentacle contraction in Discophrya collini: the effects of ionophore A23187 and ruthenium red on Ca^{2+}-induced contraction and uptake of extracellular calcium. Protoplasma 122: 125-131.

Baloun, J. and J. Hudak. 1979. Nuclear degeneration induced by chlortetracycline. Experientia 35: 201-202.

Bar-Sagi, D. and J. Prives. 1983. Trifluoperazine, a calmodulin antagonist, inhibits muscle cell function. J. Cell Biol. 97: 1375-1380.

Blinks, J.R., W.G. Wier, P.Hess and F.G. Prendergast. 1982. Measurement of Ca^{2+} concentrations in living cells. Prog. Biophys. Molec. Biol. 40: 1-114.

Blum, J.L. 1971. Notes on American Vaucheriae. Bull. Torr. Club 98: 189-194.

Blum, J.L. 1972. North American Flora; Vaucheriaceae N. Am. Flora II. 8: 1-64. New York Botanical Gardens, New York.

Bold, H.C. and M.J. Wynne. 1985. Introduction to the Algae. Vol. 2. Prentice-Hall, Inc., New Jersey. pp. xvi + 720.

Boss, W.F., H.D. Grimes and A. Brightman. 1984. Calcium-induced fusion of fusogenic wild carrot protoplasts. Protoplasma 120: 209-215.

Briarty, L.G. 1980. Stereological analysis of cotyledon cell development in Phaseolus. J. Exp. Bot. 31: 1379-1386.

Buckhout, T.J. 1984. Characterization of Ca^{2+} transport in purified endoplasmic reticulum vesicles from Lepidium sativum L. roots. Plant Physiol. 76: 962-967.

Buller, A.H.R. 1958. Researches on Fungi. vol. 5. pp. 75-167. Hafner, New York.

Burns, A.R., L. Oliveira and T. Bisalputra. 1982. A morphological study of bud initiation in the brown alga Sphacelaria furcigera. New Phytol. 92: 309-325.

Burns, A.R., L. Oliveira and T. Bisalputra. 1984. A cytochemical study of cell wall differentiation during bud initiation in the brown alga Sphacelaria furcigera. Bot. Mar. 27: 45-54.

Burr, F.A. and J.A. West. 1970. Light and electron microscope observations on the vegetative and reproductive structures of Bryopsis hypnoides. Phycologia 9: 17-37.

Caswell, A.H. 1979. Methods of measuring intracellular calcium. Int. Rev. Cyt. 56: 145-181.

Chandler, D.E. and J.A. Williams. 1978a. Intracellular divalent cation release in pancreatic acinar cells during stimulus-secretion coupling. I. Use of chlorotetracycline as a fluorescent probe. J. Cell Biol. 76: 371-385.

Chandler, D.E. and J.A. Williams. 1978b. Intracellular divalent cation release in pancreatic acinar cells during stiumlus-secretion coupling II. Subcellular localization of the fluorescent probe chlorotetracycline. J. Cell Biol. 76: 386-399.

Chen, T-H. and L.F. Jaffe. 1979. Forced calcium entry and polarized growth of Funaria spores. Planta 144: 401-406.

Chopra, G.L. 1971. A Text Book of Algae. S. Nagin Sales Corp. Delhi. pp. 328.

Christensen, T. 1969. Vaucheria collections from Vaucher's region. Biol. Skr. 16: 1-36.

Christensen, T. 1980. Algae: A Taxonomic Survey. Univ. of Copenhagen. AiO Tryk as, Odense. pp. 216.

Cole, K. and R.G. Sheath. 1980. Ultrastructural changes in major organelles during spermatial differentiation in Bangia (Rhodophyta). Protoplasma 102: 253-279.

Dangeard, P. 1939. Le genre Vaucheria, specialement dans la region du sud-ouest de la France. Le Botaniste 29: 183-265.

De Mey, Y., M. Moeremaus, G. Geuens, R. Nuydens, H. VanBelle and M. de Brabender. 1980. Immunocytochemical evidence for the association of calmodulin with microtubules of the mitotic apparatus. In. M. de Brabender and Y. De Mey, [eds], Microtubules and microtubule inhibitors. Amsterdam: Elsevier/North-Holland Biomedical Press, pp. 227-241.

Descomps, S. 1963a. Contribution a l'etude infrastructurale des Vaucheries (Xanthophycees, Chromophytes). Comptes Rendus Acad. Sci. Paris 256: 1333-1335.

Descomps, S. 1963b. Observations sur l'infrastructure de l'enveloppe des chloroplastes des Vaucheries (Xanthophycees). Comptes Rendus Acad. Sci. Paris 257: 727-729.

Fitch, R.S. and L. Oliveira. 1986a. Ultrastructure of aplanosporogenesis in the brackish-water alga Vaucheria longicaulis var. macounii (Blum) [Tribophyceae]. Bot. Mar. 29: 105-115.

Fitch, R.S. and L. Oliveira. 1986b. A morphometric and ultrastructural study of aplanospore release and germination in Vaucheria longicaulis var. macounii. (Can. J. Bot., submitted).

Foder, B., U. Skibsted and O. Scharff. 1984. Effect of trifluoperazine, compound 48/80, TMB-8 and verapamil on ionophore A23187 mediated calcium uptake in ATP depleted human red cells. Cell Calcium 5: 441-450.

Fritsch, R.E. 1935. The Structure and Reproduction of the Algae Vol. I. University Press, Cambridge. pp. 791.

Garbary, D.J. and R.S. Fitch. 1984. Some brackish species of Vaucheria (Tribophyceae) from British Columbia and northern Washington. Le Naturaliste Canadien 111: 125-130.

Garraway, M.D. and R.C. Evans. 1984. Fungal Nutrition and Physiology. John Wiley and Sons, Inc., New York. pp. vii + 401.

Glowacka, S.K., A. Sobata and A Przelecka. 1985. Displacement of cell-surface associated calcium inhibits phagocytosis and Ca-ATPase activity in Amoeba. Cell Biol. Intl. Repts. 9: 183-191.

Goodwin, B.C. and L.E.H. Trainor. Tip and Whorl morphogenesis in Acetabularia by calcium-regulated strain fields. J. Theor. Biol. 117: 79-106.

Greenwood, A.D. 1959. Observations on the structure of the zoospores of Vaucheria II. J. Exp. Bot. 10: 55-68.

Greenwood, A.D., I. Manton and B. Clarke. 1957. Observations on the structure of the zoospores of Vaucheria. J. Exp. Bot. 8: 71-86.

Grimes, H.D. and W.F. Boss. 1985. Intracellular calcium and calmodulin involvement in protoplast fusion. Plant Physiol. 79: 253-258.

Grotha, R. 1983. Chlorotetracycline-binding surfacd regions in gemmalings of Riella helicophylla. Planta 158: 473-481.

Harold, R.L. and F.M. Harold. 1986. Ionophores and cytochalasins modulate branching in Achlya bisexualis. J. Gen. Micro. 132: 213-219.

Hausser, I. and W. Herth. 1983. The Ca^{2+}-chelating antibiotic chlorotetracycline (CTC), disturbs multipolar tip growth and primary wall formation in Micrasterias. Protoplasma 117: 167-173.

Heath, I.B. and A.D. Greenwood. 1971. Ultrastructural observations on the kinetosomes, and golgi bodies during the asexual life cycle of Saprolegnia. Z. Zellforsch. 112: 371-389.

Hepler, P.K. and R.O. Wayne. 1985. Calcium and plant development. Ann. Rev. Plant Physiol. 36: 397-439.

Herth, W. 1978. Ionophore A23187 stops tip growth, but not cytoplasmic streaming, in pollen tubes of Lilium longiflorum. Protoplasma 96: 275-282.

Hibberd, D.J. 1980. Xanthophytes. In: (E.R. Cox, ed.), Phytoflagellates. Developments in Marine Biology, Vol. 2. Elsevier/North-Holland, New York. pp. 243-271.

Hoppaugh, K.W. 1930. Taxonomic study of species of Vaucheria collected in California. Am. J. Bot. 17: 329-347.

Horwitz, S.B. G.H. Chia, C. Marracksingh, S. Orlow, S. Pifko-Hirst, J. Schneck, L. Sorfara, M. Speaker, E.W. Wilk and O.M. Rosen. 1981. Trifluoperazine inhibits phagocytosis in a macrophagelike cultured cell line. J. Cell Biol. 91: 798-802.

Howard, R.J. and J.R. Aist. 1980. Cytoplasmic microtubules and fungal morphogenesis: Ultrastructural effects of methyl benzimidazole-2-ylcarbamate determined by freeze-substitution of hyphal tip cells. J. Cell Biol. 87: 55-64.

Irving, H.R., J.M. Griffith and B.R. Grant. 1984. Calcium efflux associated with encystment of Phytophthora palmivora zoospores. Cell Calcium 5: 487-500.

Jaffe, L.A., M.J. Weisenseel and L.F. Jaffe. 1975. Calcium accumulations within the growing tips of pollen tubes. J. Cell Biol. 67: 488-492.

Jao, C-C. 1937. New marine algae from Washington. Pap. Mich. Acad. Sci. 22: 99-116.

Kataoka, H. 1982. Colchicine-induced expansion of Vaucheria cell apex, alteration from isotropic to transversally anisotropic growth. Bot. Mag. Tokyo 95: 317-330.

Kauss, H. and U. Rausch. 1984. Compartmentation of Ca^{2+} and its possible role in volume regulation in Poterioochromonas. In: (W. Wiessner, D. Robinson and R.C. Starr, eds.), Compartments in algal cells and their interaction. Springer-Verlag Berlin Heidelberg. pp. 147-156.

Keith, C. M. di Paola, F.R. Maxfield and M.L. Shelanski. 1983. Microinjection of Ca^{2+}-calmodulin causes a localized depolymerization of microtubules. J. Cell Biol. 97: 1918-1924.

Kiermayer, O. and U. Meindl. 1984. Interaction of the golgi apparatus and the plasmalemma in the cytomorphogenesis of Micrasterias. In: (W. Wiessner, D. Robinson and R.C. Starr, eds.), Compartments in algal cells and their interaction. Springer-Verlag, Berlin Heidelberg. pp. 175-182.

Knutzen, J. 1973. Marine species of Vaucheria in Southern Norway. Norwegian J. Bot. 20: 163-181.

Koch, W.I. 1951. A study of the motile cells of Vaucheria. J. Elisha Mitchell Sci. Soc. 67: 123-131.

La Claire II, J.W. 1983. Inducement of wound motility in intact giant algal cells. Exp. Cell. Res. 145: 63-70.

La Claire II, J.W. 1984. Cell motility during wound healing in giant algal cells: contraction in detergent-permeabilized cell models in Ernodesmis. Euro. J. Cell Biol. 33: 180-189.

Lee, R.E. 1980. Phycology. Cambridge University Press, Cambridge. pp. x + 478.

Lehtonen, J. 1984. The significance of Ca^{2+} in the morphogenesis of Micrasterias studied with EGTA, verapamil, $LaCl_3$ and calcium ionophore A23187. Plant Sci. Letters 33: 53-60.

Lewin, J. 1966. Silicon metabolism in diatoms V. Germanium dioxide, a specific inhibitor of diatom growth. Phycologia 6: 1-12.

Lonergau, T.A. 1984. Regulation of cell shape in Euglena gracilis. II. The effects of altered extra- and intracellular Ca^{2+} concentrations and the effect of calmodulin antagonists. J. Cell Sci. 71: 37-50.

Marchant, H.J. 1972. Pyrenoids of *Vaucheria woroniniana* Heering. *Br. Phycol. J.* *7*: 81-84.

Marmé, D. 1985. The role of calcium in the cellular regulation of plant metabolism. *Physiol. Veg.* *23*: 945-953.

McKerracher, L.J. and I.B. Heath. 1986. Polarized cytoplasmic movement and inhibition of saltations induced by calcium-mediated effects of microbeams in fungal hyphae. *Cell Motility and the Cytoskeleton* *6*: 136-145.

Meindl, U. 1982. Local accumulation of membrane-associated calcium according to cell pattern formation in *Micrasterias denticulata*, visualized by chlorotetracycline fluorescence. *Protoplasma* *110*: 143-146.

Moestrup, O. 1970. Fine structure of spermatozoids of Vaucheria sescuplicaria and on the later stages in spermatogenesis. J. Mar. Bio. Assoc. U.K. 50: 513-523.

Moestrup, O. and L.R. Hoffman. 1973. Ultrastructure of the green alga Dichotomosiphon tuberosus with special reference to the occurrence of striated tubules in the chloroplast. J. Phycol. 9: 430-437.

Ott, D.W. 1979. Endosymbiotic bacteria in Vaucheria: association with cytoplasmic microtubules in Vaucheria sessilis. Cytobios 24: 185-194.

Ott, D.W. and R.M. Brown. 1972. Light and electron microscopic observations on mitosis in Vaucheria. Br. Phycol. J. 7: 361-374.

Ott, D.W. and R.M. Brown. 1974a. Developmental cytology of the genus Vaucheria. I. Organization of the vegetative filament. Br. Phycol. J. 9: 111-126.

Ott, D.W. and R.M. Brown. 1974b. Developmental cytology of the genus Vaucheria. II. Sporogenesis in V. fontinalis (L.) Christensen. Br. Phycol. J. 9: 333-351.

Ott, D.W. and R.M. Brown. 1975. Developmental cytology of the genus Vaucheria. III. Emergence, settlement and germination of the mature zoospore of V. fontinalis (L.) Christensen. Br. Phycol. J. 10: 49-56.

Ott, D.W. and R.M. Brown. 1978. Developmental cytology of the genus Vaucheria. IV. Spermatogenesis. Br. Phycol. J. 13: 69-85.

Papahadjopoulos, D. 1978. Calcium-induced phase changes and fusion in natural and model membranes. In: (G. Poste, G.L. Nicolson, eds.), Membrane fusion. Elsevier, New York. pp. 765-790.

Pecora, R.A. 1979. Ecology and spatial distribution of three species of Vaucheria. J. Phycol. 15: Supp. p. 21.

Pickett-Heaps, J.D. 1977. Cell division and evolution of branching in Oedocladium (Chlorophyceae). Cytobiologie 14: 319-337.

Picton, J.M. and M.W. Steer. 1982. A model for the mechanism of tip extension in pollen tubes. J. Theor. Biol. 98: 15-20.

Picton, J.M. and M.W. Steer. 1985. The effects of ruthenium red, lanthanum, fluorescein isothiocyanate, and trifluoperazine on vesicle transport, vesicle fusion and tip extension in pollen tubes. Planta 163: 20-26.

Polito, V.S. 1985. Intracellular calcium dynamics and plant cell functions. In: (H. Hidaka and D.J. Hartshorne, eds.), Calmodulin antagonists and cellular physiology. Academic Press, Inc., Orlando, Florida. pp. 457-467.

Pomeroy, W.M. 1977. Benthic algal ecology and primary pathways of energy flow in the Squamish River delta, British Columbia. PhD. thesis, University of British Columbia. 175 p.

Pomeroy, W.M. and J.G. Stockner. 1976. Effects of environmental disturbance on the distribution and primary production of benthic algae on a British Columbia estuary. J. Fish. Res. Bd. Can. 33: 1175-1187.

Pringsheim, N. 1855. Uber die Befruchtung der Algen. Preuss. Akad. der Wiss. Berl. Monatsber. Ges. 1: 133-165.

Pueschel, C.M. 1979. Ultrastructure of tetrasporogenesis in Palmaria palmata (Rhodophyta). J. Phycol. 15: 409-424.

Quatrano, R.S. 1978. Development of cell polarity. Ann. Rev. Plant Physiol. 29: 487-510.

Reed, P.W. and M.A. Lardy. 1972. A23187: a divalent cation ionophore. J. Biol. Chem. 247: 6970-6977.

Reiss, H-D. and W. Herth. 1978. Visualization of the Ca^{2+}-gradient in growing pollen tubes of Lilium longiflorum with chlorotetracycline fluorescence. Protoplasma 97: 373-377.

Reiss, H-D. and W. Herth. 1979a. Calcium ionophore A23187 affects localized wall secretion in the tip region of pollen tubes of *Lilium longiflorum*. *Planta* **145**: 225-232.

Reiss, H-D. and W. Herth. 1979b. Calcium gradients in tip growing plant cells visualized by chlorotetracycline fluorescence. *Planta* **146**: 615-621.

Reiss, H-D. and W. Herth. 1982. Disoriented growth of pollen tubes of *Lilium longiflorum* Thunb. induced by prolonged treatment with the calcium-chelating antibiotic chlorotetracycline. *Planta* **156**: 218-225.

Reiss, H-D. and W. Herth. 1985. Nifedipine-sensitive calcium channels are involved in polar growth of lily pollen tubes. *J. Cell Sci.* **76**: 247-254.

Reiss, H-D, W. Herth and R. Nobiling. 1985. Development of membrane- and calcium gradients during pollen germination of *Lilium longiflorum*. *Planta* **163**: 84-90.

Reiss, H-D., W. Herth and E. Schnepf. 1983. The tip-to-base calcium gradient in pollen tubes of Lilium longiflorum measured by proton-induced X-ray emission (PIXE). Protoplasma 115: 153-159.

Reynolds, E.S. 1963. The use of lead citrate at high pH as an electron-opaque stain in electron microscopy. J. Cell Biol. 17: 208-212.

Rieth, A. 1980. Xanthophyceae. Susswasserflora von Mitteleuropa Band 4: Rieth. Xanthophyceae 2. Teil. Gustav Fischer Verlag, Stuttgart, New York. pp. xiv + 147.

Saunders, M.J. 1986. Cytokinin activation and redistribution of plasma-membrane ion channels in Funaria. Planta 167: 402-409.

Saunders, M.J. and P.K. Hepler. 1981. Localization of membrane-associated calcium following cytokinin treatment in Funaria using chlorotetracycline. Planta 152: 272-281.

Scagel, R.F. 1957. An annotated list of the marine algae of British Columbia and northern Washington. Bull. Nat. Mus. Can. no. 150. 289 pp.

Schliwa, M., U. Euteneuer, J.C. Bulinski and J.G. Izant. 1981. Calcium lability of cytoplasmic microtubules and its modulation by microtubule-associated proteins. Proc. Nat. Acad. Sci. U.S.A. 78: 1037-1041.

Schmeidel, G. and E. Schnepf. 1980. Polarity and growth of caulonema tip cells of the moss Funaria hygrometrica. Planta 147: 405-413.

Schmitz, F. 1878. Untersuchungen uber die Zellkerne der Thallophyten. Sber. niederr. Ges. Bonn. pp. 345-349.

Schnepf, E. 1986. Cellular polarity. Ann. Rev. Plant Physiol. 37: 23-47.

Schnepf, E., B. Hrdina and A. Lehne. 1982. Spore germination, development of the microtubule system and protonema cell morphogenesis in the moss, Funaria hygrometrica: effects of inhibitors and growth substances. Biochem. Physiol. Pflanzen 177: 461-482.

Scott, J. 1983. Mitosis in the freshwater red alga Batrachospermum ectocarpum. Protoplasma 118: 56-70.

Sievers, A. and E. Schnepf. 1981. Morphogenesis and polarity of tubular cells with tip growth. In (O. Kiermayer, ed.), Cytomorphogenesis in plants. Springer-Verlag, Wien, New York. pp. 265-299.

Simons, J. 1974. Vaucheria compacta: a euryhaline estuarine algal species. Acta. Bot. Neerl. 23: 613-626.

Simons, J. 1975. Vaucheria sp. from estuarine areas in the Netherlands. Neth. J. Sea Res. 9: 1-23.

Skibsted, U., B. Foder and O. Scharff. 1984. Effect of trifluoperazine, compound 48-80 and verapamil on ionophore A23187 induced calcium transients in human red cells. Cell Calcium 5: 451-462.

Smedley, M. and M. Stanisstreet. 1985. Effect of calmodulin inhibitors on would healing in Xenopus early embryos. Cytobios 42: 25-32.

Smith, G.M. 1950. The Fresh-Water Algae of the United States. 2nd ed., McGraw-Hill Book Co., New York. pp. vii + 719.

Strasburger, E. 1880. Zellbildung und Zelltheilung. 3rd ed. Jena.

Strasburger, E. 1890. Reduktionsteilung, Spindelbildung, Centrosomen und Cilienbildner im Pflanzenreich. Histol. Beitr. 6: 187-190.

Taylor, W.r. 1952. Notes on Vaucheria longicaulis (Hoppaugh). Madrono 11: 274-277.

Thuret, G. 1843. Recherches sur les organes locomoteurs des spores des algues. Annls. Sci. nat. (Bot.) Ser. II 19: 266-277.

Trentepohl, J.F. 1807. Beobachtung uber die Fortpflanzung der Ectospermen des Herrn Vaucher, insonderheit der Conferva bullosa Linn. nebst einigen Bemerkungen uber die Oscillatorien. In: Bot Bemerkungen und Berichtigungen von A.W. Roth, Leipzig. pp. 180-216.

Turner, J.B. and E.I. Friedmann. 1974. Fine structure of capitular filaments in the coenocytic green alga Penicillus. J. Phycol. 10: 125-131.

Unger, F. 1843. Die Pflanze im Momente der Thierwerdung. Vienna.

van Adelsberg, J. and Q. Al-Awqati. 1986. Regulation of cell pH by Ca^{2+}-mediated exocytosis insertion of H^{+}-ATPases. J. Cell Biol. 102: 1638-1645.

Vaucher, J.P. 1801. Memoire sur les graines des Conferves. J. Phys. Chim. Hist. nat et Arts LII: 344-359.

Venkataraman, G.S. 1961. Vaucheriaceae. Indian Council of Agri. Res., New Delhi. pp. ix + 112.

Vesk, M. and M.A. Borowitzka. 1984. Ultrastructure of tetrasporogenesis in the coralline alga Haliptilon cuvieri (Rhodophyta). J. Phycol. 20: 501-515.

Volberg, T., B. Geiger, J. Kartenbeck and W.W. Franke. 1986. Changes in membrane-microfilament interaction in intercellular adherens junctions upon removal of extracellular Ca^{2+} ions. J. Cell Biol. 102: 1832-1842.

Wayne, R. and P.K. Hepler. 1985. Red light stimulates an increase in intracellular calcium in the spores of Onoclea sensibilis. Plant Physiol. 77: 8-11.

Weibel, E.R. 1973. Stereological techniques for electron microscopic morphometry. In: (M.A. Hayat, ed.), Principles and techniques of electron microscopy: Biological applications. Vol. 3. Von Nostrand Rheinhold Co., New York.

Weisenseel, M.H. and R.M. Kicherer. 1981. Ionic currents as control mechanisms in cytomorphogenesis. In: (O. Kiermayer, ed.), Cytomorphogenesis in plants. Springer-Verlag, Wien, New York. pp. 379-399.

Wise, D. and S.M. Wolniak. 1984. A calcium-rich intraspindle membrane system in spermatocytes of wolf spiders. Chromosoma (Berl.) 90: 156-161.

Wolniak, S.M., P.K. Hepler and W.T. Jackson. 1980. Detection of the membrane-calcium distribution during mitosis in Haemanthus endosperm with chlorotetracycline. J. Cell Biol. 87: 23-32.

Woods, C.M., M.S. Reid, and B.D. Patterson. 1984. Response to chilling stress in plant cells I. Changes in cyclosis and cytoplasmic structure. Protoplasma 121: 8-16.